JOURNAL OF GEOPHYSICAL RESEARCH, VOL. 97, NO. B5, PAGES 6849–6866, MAY 10, 1992

Petrology, Elasticity, and Composition of the Mantle Transition Zone

JOEL ITA AND LARS STIXRUDE[1]

Department of Geology and Geophysics, University of California, Berkeley

We compare the predictions of compositional models of the mantle transition zone to observed seismic properties by constructing phase diagrams in the MgO-FeO-CaO-Al_2O_3-SiO_2 system and estimating the elasticity of the relevant minerals. Mie-Grüneisen and Birch-Murnaghan finite strain theory are combined with ideal solution theory to extrapolate experimental measurements of thermal and elastic properties to high pressures and temperatures. The resulting thermodynamic potentials are combined with the estimated phase diagrams to predict the density, seismic parameter, and mantle adiabats for a given compositional model. We find that the properties of pyrolite agree well with the observed density and bulk sound velocity of the upper mantle and transition zone. Piclogite significantly underestimates the magnitude of the 400-km velocity discontinuity and overestimates the velocity gradient in the transition zone. Substantially enriching piclogite in Al provides an acceptable fit to the observations. Invoking a chemical boundary layer between the uppermost mantle and transition zone leads to poor agreement with observed seismic properties for the compositions considered. Within the transition zone, the dissolution of garnet to Ca-perovskite near 18 GPa may explain the proposed 520-km seismic discontinuity. Below 700 km depth, all compositions disagree with observed bulk sound velocities, implying that the lower mantle is chemically distinct from the upper mantle.

INTRODUCTION

The transition zone between the upper and lower parts of the Earth's mantle has been recognized through seismic observations for some time, but its composition and the mineralogical changes responsible for its boundaries, the two largest velocity discontinuities in the mantle, are still uncertain. The thermal and chemical evolution of the Earth depends critically on whether the transition zone is bounded by phase changes alone or by changes in phase and composition. While the former is consistent with whole mantle convection, the latter requires convection in at least three layers, which greatly reduces the efficiency of chemical mixing and heat transport. Multiple convective layers imply a slowly evolving Earth, one which has readily preserved large-scale chemical heterogeneities and retained most of its primordial heat.

Some models of the early evolution of the Earth suggest strong chemical fractionation and the formation of multiple compositional layers. These models, which are based on analogy with crustal magma chambers, envision silicate liquids sinking relative to lighter olivine in the shallow mantle but rising relative to denser perovskite in the lower mantle, producing a chemically distinct transition zone [*Anderson and Bass*, 1986; *Ohtani*, 1988]. However, detailed analysis of very high Rayleigh number dynamics indicates that convective mixing in a planet scale magma chamber may completely prevent crystal fractionation [*Tonks and Melosh*, 1990]. Furthermore, extensive crystal fractionation appears inconsistent with the Earth's trace element chemistry [*Kato et al.* [1988], but see also *Walker and Agee* [1989]).

Different classes of geophysical observations are most easily explained by either single- or multiple-layer models of mantle convection, but nearly all data currently available permit several interpretations. The inferred penetration of subducting slabs into, and in some cases through, the transition zone is easily accommodated by whole mantle convection models but cannot rule out substantial chemical stratification imposed by semipermeable (leaky) transition zone boundary layers [*Isacks and Molnar*, 1971; *Jarrard*, 1986; *Creager and Jordan*, 1984, 1986; *Silver and Chan*, 1986]. Some slabs are apparently prevented from reaching the lower mantle and are significantly deformed by its upper boundary, suggesting a substantial change in material properties at 660 km depth and a stratified mantle [*Giardini and Woodhouse*, 1984; *Zhou and Clayton*, 1990]. A tenfold to 30-fold increase in viscosity at 660 km depth, which does not require multiple-layer convection or compositional layering, may also explain slab deformation and is independently inferred from geoid observations [*Vassiliou et al.*, 1984; *Hager and Richards*, 1989]. At the same time, the absence of slab deformation at 400 km is not inconsistent with compositional change at that boundary provided the attendant changes in density and viscosity are not large enough to significantly impede the slab's descent. Many geochemical observations are most easily explained by the survival of two or more physically distinct reservoirs, such as multiple convective layers [*DePaolo*, 1983; *Allègre and Turcotte*, 1985; *Zindler and Hart*, 1986; *Silver et al.*, 1988]. However, inefficient mixing in the present mantle may allow the long-term survival of chemical heterogeneity on many length scales even in single-layer convection [*Davies*, 1984; *Gurnis and Davies*, 1986].

Comparison of seismic observations of the Earth's interior with known material properties is the most direct way of determining the transition zone's composition. The region's extreme petrologic complexity, however, has severely hindered past efforts. It was first recognized by *Birch* [1952] that the anomalously high seismic velocity gradients in the transition zone were most easily explained by a series of pressure-induced phase transformations, rather than the effect of pressure on a single phase. The rapid development

[1]Now at Center for High Pressure Research, Geophysical Laboratory, Carnegie Institution of Washington, Washington, D.C.

Paper number 92JB00068.
0148-0227/92/92JB-00068$05.00

TABLE 1. Chemical Composition

	Pyrolite, mol %	Piclogite, mol %
SiO_2	38.29	41.94
MgO	49.33	42.32
FeO	6.27	5.29
CaO	3.27	8.67
Al_2O_3	2.22	1.78
Na_2O	0.33	...
Cr_2O_3	0.15	...
Ti_2O	0.14	...
100 × MgO/MgO + FeO	88.72	88.88
$(Mg, Fe)_2SiO_4$ %	62	40
Si #[a]	3.23	3.46

[a] Si # is number of Si atoms per every 12 O atoms.

of experimental high-pressure metamorphic petrology in the last few years has revealed that as many as 25 different mineral species may be present in the transition zone. Partly because the elastic properties and phase stability of many important minerals have been measured only recently, previous studies, which were forced to rely on estimates of these quantities, came to very different conclusions [*Bina and Wood*, 1987; *Weidner and Ito*, 1987; *Irifune*, 1987; *Duffy and Anderson*, 1989].

We analyze two competing models of transition zone composition, pyrolite and piclogite, by combining a consistent thermodynamic formulation with recent measurements of mineral elasticity and phase equilibria. The two compositional models, originally proposed in the context of one- and three-layer models of mantle convection, respectively, have very different consequences for the state of the Earth's interior. The development of these two models is discussed by *Ringwood* [1975], *Anderson and Bass* [1984], *Irifune and Ringwood* [1987*a*], and *Duffy and Anderson* [1989].

We define the compositional models below and synthesize experimental petrologic data by constructing summary phase diagrams for each composition. We then describe the semiempirical thermodynamic potential formalism which allows self-consistent determination of density, bulk modulus, and adiabats throughout the pressure-temperature regime of the Earth's mantle. By focusing on comparisons with the density and bulk sound velocity of the mantle, we are able to base our conclusions only on measured mineral properties. We estimate the bounds which seismic observations place on transition zone composition and discuss their geophysical implications.

Composition and Phase Equilibria

Table 1 lists the compositions of pyrolite [*Irifune*, 1987] and piclogite [*Duffy and Anderson*, 1989] used here. To fully exploit experimental results on simple pseudobinary systems, we assume that these bulk compositions can be separated into two subsystems, olivine and the remainder (residuum, Table 2) which do not affect each other's phase equilibria (see also *Jeanloz and Thompson* [1983] and *Irifune* [1987]). This is consistent with the results of *Akaogi and Akimoto* [1979] which show no change in the relative proportions of these two subsystems to at least 20 GPa.

We base the form of the $(Mg,Fe)_2SiO_4$ phase diagram on the experiments of *Ito and Takahashi* [1989] and *Katsura and Ito* [1989] (Figure 1). These data along with the thermochemical calculations of *Akaogi et al.* [1989], *Wood* [1990], and *Fei et al.* [1991] provide tight constraints on the relevant phase boundaries (precision of ±0.5 GPa) throughout the pressure-temperature range considered here. We use the same phase diagram for both pyrolite and piclogite since they have nearly identical magnesium to iron ratios.

Phase diagrams in the residuum component (Figure 2) are primarily constrained by measurements on the Mg, Fe, and (Ca,Mg) pyroxene-garnet joins up to 20 GPa reviewed by *Akaogi et al.* [1987] and the enstatite-pyrope join from 24 to 27 GPa [*Kanzaki*, 1987; *Irifune and Ringwood*, 1987*a*] and direct observation of pyrolite residuum at 1200°C throughout the pressure range considered here [*Irifune and Ringwood*, 1987*b*]. These data encompass the major element chemistries of pyrolite and piclogite (Table 2).

The coexistence field of pyroxene and garnet is perturbed slightly from its location on the enstatite-pyrope join by the competing effects of Ca and Fe substitution. Because both pyrolite and piclogite residua have more Ca than Fe, we have raised the pyroxene + garnet to garnet boundary above that in the magnesium end-member by 1 GPa, based on linear interpolation of the results of *Akaogi et al.* [1987]. Compared with pyrolite, the lower Al content of piclogite raises the boundary slightly and reduces its temperature dependence [*Akaogi et al.*, 1987]. Our estimated boundaries are consistent with the whole rock experiments of *Irifune* [1987], *Irifune and Ringwood* [1987*b*], and *Takahashi and Ito* [1987].

We assume that the formation of Ca-perovskite is not strongly dependent on bulk composition and base the garnet to garnet + Ca-perovskite transition on observed transitions in diopside and hedenbergite. Ca-perovskite first forms at 17 GPa in diopside [*Irifune et al.*, 1989; *Tamai and Yagi*, 1989] and at somewhat higher pressures in more Fe rich compositions [*Kim et al.*, 1989]. Assuming that Fe has a linear effect on the appearance of Ca-perovskite, we place the garnet to garnet + Ca-perovskite transition at 18 GPa. This estimate is consistent with observations of pyrolite residuum by *Ito and Takahashi* [1987*a*] and *Irifune* [1987] and of complete pyrolite by *Takahashi and Ito* [1987]. These experiments indicate that the boundary is insensitive to temperature.

Above 18 GPa, our estimated phase boundaries are identical to those in the enstatite-pyrope system as determined by *Kanzaki* [1987] and *Irifune and Ringwood* [1987*a*]. This is supported by the observed garnet + Ca-perovskite to garnet + (Mg,Fe)-perovskite + Ca-perovskite boundary in pyrolite residuum [*Ito and Takahashi*, 1987*a*; *Irifune and Ringwood*, 1987*b*] which agrees with the garnet to garnet +

TABLE 2. Residuum Composition

	Pyrolite, mol %	Piclogite, mol %
SiO_2	48.60	48.39
MgO	29.93	29.64
FeO	3.82	3.71
CaO	9.45	15.17
Al_2O_3	6.40	3.11
Na_2O	0.95	...
Cr_2O_3	0.44	...
Ti_2O	0.42	...
Si #	3.58	3.76

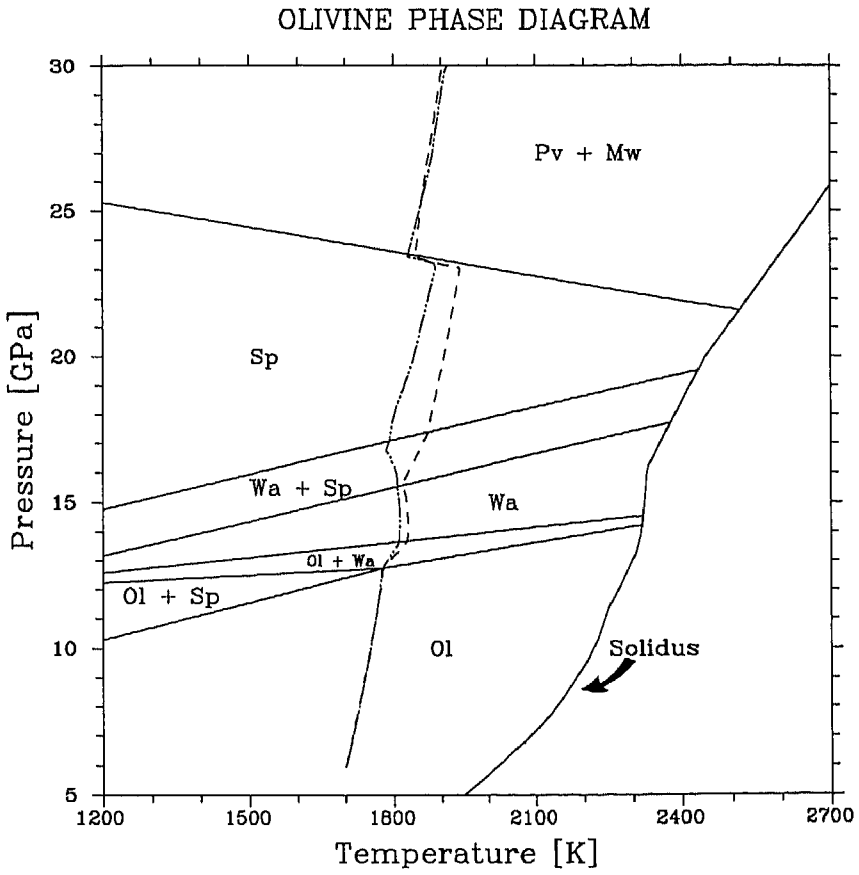

Fig. 1. $(Mg,Fe)_2SiO_4$ phase diagram. The mantle solidus is from *Ito and Takahashi* [1987*b*] and *Gasparik* [1990]. The 1700°K adiabats of pyrolite (dashed line) and piclogite (dot-dashed line) are superimposed (see text and Figure 3).

(Mg,Fe)-perovskite boundary on the enstatite-pyrope join [*Irifune and Ringwood*, 1987*a*]. The inferred formation of ilmenite from pyrolite residuum [*Irifune and Ringwood*, 1987*b*] also agrees with our estimated phase boundaries. Compared with pyrolite, the lower Al content of piclogite extends the stability of ilmenite to slightly higher temperatures. The assumed lower mantle assemblage is in excellent agreement with very high pressure (25–84 GPa) determinations of peridotite phase equilibria [*O'Neill and Jeanloz*, 1990].

On the basis of the results of *Akaogi and Akimoto* [1977], olivine and residuum systems are assigned identical bulk Fe contents. Volume fractions and Fe contents of coexisting phases in the olivine system are determined by the phase diagrams of *Katsura and Ito* [1989] and *Ito and Takahashi* [1989] and the pressure- and temperature-independent Mg-Fe partition coefficient between magnesiowüstite and perovskite from *Fei et al.* [1991].

In the residuum component, volume fractions and Al contents of coexisting pyroxene and garnet are taken from the phase diagrams of *Akaogi et al.* [1987], which are consistent with the results of *Irifune and Ringwood* [1987*a*, *b*]. We ignore the effects of Al on the properties of enstatite since only minor amounts (less than 1%) are soluble at the pressures of interest here. Pressure- and temperature-independent Mg-Fe partition coefficients between pyroxene and garnet are taken from *Akaogi and Akimoto* [1979]. The results of *Irifune* [1987] and *Irifune and Ringwood* [1987*a*, *b*] on pyrolite and harzburgite compositions determine the amount of Ca-perovskite. Volume fractions and Al contents of coexisting garnet and perovskite are determined by the phase diagram of *Irifune and Ringwood* [1987*a*]. In the absence of data, we have assumed an Mg-Fe partition coefficient of unity between garnet and (Mg,Fe)-perovskite.

THERMODYNAMICS AND ELASTICITY

Calculations of mineral elasticity and mantle adiabats are self-consistently based on a semiempirical thermodynamic potential formalism. The Gibbs free energy G of a phase consisting of a solid solution of N species as a function of pressure P and temperature T is [e.g., *Guggenheim*, 1952]

$$G(P, T) = \sum_{i=1}^{N} x_i[G_i(P, T) + RT \ln a_i] \quad (1)$$

where

$$G_i(P, T) = F_i(V, T) + PV_i \quad (2)$$

is the Gibbs free energy of a single species (end-member), a_i, F_i, and V_i are its activity, Helmholtz free energy, and molar volume, respectively, and R is the gas constant. We assume that the quantity $RT \ln f_i$, where the activity coefficient (f_i is defined by $a_i = f_i x_i$) is independent of pressure and temperature (see also, for example, *Wood* [1990]). This is equivalent to the assumption of ideal behavior for all of the thermodynamic properties of interest here (first- and higher-

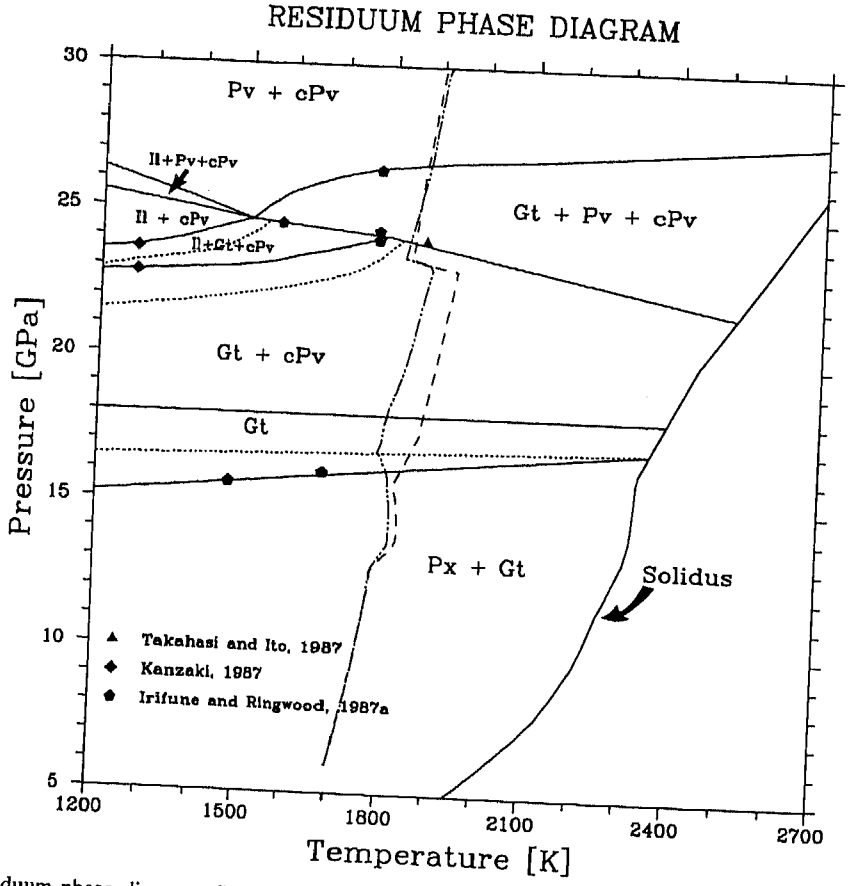

Fig. 2. Residuum phase diagram. Symbols present experimental observations of phase boundaries. Solid lines represent phase boundaries in pyrolite. Where piclogite differs from pyrolite, its phase boundaries are represented by dotted lines. Mantle solidus is the same as in Figure 1. The 1700°K adiabats of pyrolite (dashed line) and piclogite (dot-dashed line) are superimposed (see text and Figure 3). Px = Opx + Cpx; Gt = Py + Gr + Maj + Ca-Maj.

order pressure and temperature derivatives of G). Deviations from ideality are well documented in silicates [e.g., *Saxena*, 1973], but the effects on properties deduced from seismic observations are small compared with other uncertainties in mineralogical and seismic data. The deviation of molar volumes from ideal behavior at zero pressure (as much as 0.2%) is similar to the precision of high-pressure volume determinations and substantially smaller than the uncertainties in observed mantle densities (see the review of *Jeanloz and Thompson* [1983] and the more recent work of *Hazen et al.* [1990] and *Mao et al.* [1991] on Mg-Fe solutions, *Ohashi and Finger* [1976] and *Ohashi et al.* [1975] on the effect of Ca and the discussion of the molar volumes of garnet-majorite solutions below). Available data on the bulk modulus of intermediate compositions considered here are consistent with ideal behavior [*Jeanloz and Thompson*, 1983; *Richet et al.*, 1989; *O'Neill et al.*, 1989; *Hazen et al.*, 1990]. Excess entropies of mixing are much smaller than the ideal mixing term in Mg-Fe solutions [e.g., *Wood and Kleppa*, 1981] but can be of comparable magnitude if the radii of cations occupying the mixing site differ substantially (Ca-Mg solutions) [*Haselton and Newton*, 1980]. Mixing entropies are smaller than entropy changes associated with phase transitions and contribute less than 1.2% to the total entropy. In general, variations in the entropy of mixing have a small effect on the properties considered here since their only influence is through slight changes in adiabatic temperatures.

We assume that the Helmholtz free energy of species i, F_i, can be divided into a reference part, a cold part, and a thermal part (subscript i on all material properties understood):

$$F(V, T) = F_0 + F_C(V, T_0) + [F_{TH}(V, T) - F_{TH}(V, T_0)] \quad (3)$$

where

$$F_C(V, T_0) = 9K_0V_0(f^2/2 + a_1f^3/3 + a_2f^4/4 + \cdots) \quad (4a)$$

$$f = (1/2)[(V_0/V)2/3 - 1] \quad (4b)$$

$$a_1 = (3/2)(K_0' - 4), \quad (4c)$$

$$a_2 = (3/2)[K_0K_0'' + K_0'(K_0' - 7) + 143/9] \quad (4d)$$

and

$$F_{TH} = 9nRT(T/\theta)^3\int_0^{\theta/T} \ln(1 - e^t)t^2\,dt + A_2T^2 \quad (5)$$

where K_0, K_0', and K_0'' are the isothermal bulk modulus and its first and second pressure derivatives, θ is the Debye temperature and the subscript zero indicates reference values at zero pressure and room temperature. Because strains in the transition zone are small ($f < 0.05$), we neglect fourth- and higher-order terms in (4a). Anharmonic terms

are expected to be small at the pressures and temperatures of interest here and are neglected ($A_2 = 0$) [*Hardy*, 1980; *Stixrude and Bukowinski*, 1990]. The Grüneisen parameter, $\gamma = -\partial \ln \theta / \partial \ln V$, is assumed to have the form

$$\gamma = \gamma_0 (V/V_0)^q \tag{6}$$

where we assume $q = 1 \pm 1$.

The thermodynamic potential of species i (equations (3)–(6)), most often seen in the form of the Mie-Grüneisen equation of state (subscript i on all material properties understood):

$$P = -(\partial F/\partial V)_T = 3K_0 f(1 + 2f)^{5/2}(1 + a_1 f) + (\gamma/V)[E_{\mathrm{TH}}(V, T) - E_{\mathrm{TH}}(V, T_0)] \tag{7}$$

where

$$E_{\mathrm{TH}} = 9nRT(T/\theta)^3 \int_0^{\theta/T} t^3/(e^t - 1)\, dt \tag{8}$$

has proved successful in reproducing a large body of thermodynamic data including equations of state, heat capacities, unary phase equilibria, and melting [*Shapiro and Knopoff*, 1969; *Knopoff and Shapiro*, 1969; *McQueen et al.*, 1970; *Jeanloz*, 1989; *Stixrude and Bukowinski*, 1990]. The entropy, isothermal bulk modulus, heat capacity at constant volume, and thermal expansivity of species i are given directly by (3) (subscript i on all material properties understood):

$$S = -(\partial F/\partial T)_V = 9nR(T/\theta)^3 \cdot \int_0^{\theta/T} [t/(e^t - 1) - \ln(1 - e^{-t})]t^2\, dt \tag{9}$$

$$K = V(\partial^2 F/\partial V^2) = K_0(1 + 2f)^{5/2}[1 + (7 + 2a_1)f + 9a_1 f^2] + (\gamma/V)[\gamma + 1 - q][E_{\mathrm{TH}}(V, T) - E_{\mathrm{TH}}(V, T_0)] - (\gamma^2/V)[TC_V(V, T) - T_0 C_V(V, T_0)] \tag{10}$$

$$C_V = -T(\partial^2 F/\partial T^2)_V = 9nR(T/\theta)^3 \int_0^{\theta/T} e^t t^4\, dt/(e^t - 1)^2 \tag{11}$$

$$\alpha = -(\partial^2 F/\partial V \partial T)/K = \gamma C_V/KV. \tag{12}$$

The molar volume, isothermal bulk modulus, thermal expansivity, heat capacity, entropy, and adiabatic bulk modulus of a mineral solid solution at a given pressure and temperature are given directly by (1) and the assumption, discussed above, that $RT \ln f_i$ is constant. Using the expressions for the corresponding properties of the individual species i (equations (6)–(12)), we have

$$V = (\partial G/\partial P)_T = \sum_{i=1}^{N} x_i V_i \tag{13}$$

$$K = -V/[(\partial^2 G/\partial P^2)_T] = V \Big/ \left(\sum_{i=1}^{N} x_i V_i / K_i \right) \tag{14}$$

$$\alpha = (\partial^2 G/\partial P \partial T)/V = \left(\sum_{i=1}^{N} x_i V_i \alpha_i \right) / V \tag{15}$$

$$C_V = -T \sum_{i=1}^{N} (\partial^2 F/\partial T^2)_V = \sum_{i=1}^{N} x_i C_{Vi} \tag{16}$$

$$S = -(\partial G/\partial T)_P = \sum_{i=1}^{N} x_i S_i - R x_i \ln x_i \tag{17}$$

$$K_s = K(1 + KTV\alpha^2/C_V). \tag{18}$$

Mineral properties are combined to calculate the density, entropy, and bulk sound velocity, $V_\phi = (K_s/\rho)^{1/2}$, of mantle compositions. We use the Voight-Reuss-Hill method [*Watt et al.*, 1976] to determine the bulk modulus of the polyphase aggregate, resulting in tight bounds on bulk sound velocities (±0.35% on average). Potential systematic errors in the calculation of mantle velocities arise from the assumptions of isotropy and homogeneity in this, as well as other, more restrictive bounding schemes (e.g., *Hashin and Shtrikman* [1963]; see *Watt et al.* [1976] and *Salerno and Watt* [1986]). Tomographic results show strong seismic anisotropy in the mantle above 200 km depth which decreases rapidly with depth and is unresolvable below 400 km [*Montagner and Tanimoto*, 1991]. The observed decrease of scattering attenuation with increasing earthquake depth indicates that the mantle heterogeneities on scale lengths typical of short period seismic waves (1–10 km) decreases with depth and is small below 200 km [*Korn*, 1988].

The thermodynamic potential (1) is expressed in terms of its natural variables and thus contains all thermodynamic information about the model system; it is a fundamental thermodynamic relation in the terminology of *Callen* [1985]. All thermodynamic properties are given by pressure and temperature derivatives of (1). The potential formulation has important advantages over partial descriptions such as the equation of state (P-V-T relation) which contains no information about entropy. In addition to complete self-consistency between calculated densities, bulk sound velocities, and mantle adiabats, the thermodynamic potentials used here generally require a small number of parameters since they are physically based (Eulerian finite strain theory and the Debye model of the vibrational density of states). This allows us to constrain each parameter independently by a large number of experimental measurements. In contrast, perturbative schemes, either simple polynomials in pressure and temperature or more complex forms [*Plymate and Stout*, 1989, and references therein; *Akaogi et al.*, 1989; *Duffy and Anderson*, 1989; *Fei et al.*, 1991] generally require an additional, often poorly constrained parameter for each higher-order derivative property such as the temperature dependence of K or the pressure dependence of α. The temperature derivative of the bulk modulus, for instance, which is unmeasured for nearly all mantle minerals, does not appear explicitly in our formulation but is determined by θ_0 and γ_0, which are constrained by heat capacity and thermal expansivity data.

The thermodynamic potential parameters for transition zone species are given in Table 3. The molar volumes of

TABLE 3. Parameters of the Thermodynamic Potential

Name	Formula	Abbreviation	V_0[a], cm³/mol		K_0, GPa		K_0'		θ_0, °K		γ_0	
			Value	Reference	Value	Reference	Value	Reference	Value	Reference	Value	Reference
Forsterite	Mg_2SiO_4	Ol	43.76		128	1 and 2	5.0	1 and 3	924	4 and 5	1.14	4 and 5
Fayalite	Fe_2SiO_4		46.27		127	6	5.2	6 and 7	688	8 and 9	1.08	8 and 9
Wadsleyite	Mg_2SiO_4	Wa	40.52		174	10	4.0 (4.8)	11 (12)	974	5 and 13	1.32	5 and 13
	Fe_2SiO_4		43.22		174[b]	14	4.0[b] (4.8)[b]	14	771[c]		1.32[b]	
Spinel	Mg_2SiO_4	Sp	39.65		183	15	4.1 (5.0)	16 (17)	1017	5 and 18	1.21	5 and 18
	Fe_2SiO_4		42.02		192	19	4.1 (5.0)[b]	20	805	9 and 18	1.52	9 and 18
Enstatite	$MgSiO_3$	Opx	31.33		106	21	5.0	22 and 23	935	24 and 25	0.97	24 and 25
Ferrosilite	$FeSiO_3$		32.96		101	26	5.0[b]		676	9 and 27	0.98	9 and 27
Diopside	$CaMgSi_2O_6$	Ca-Cpx	66.11	28	114	29	4.5	30	941	25 and 28	1.06	25 and 28
Hedenbergite	$CaFeSi_2O_6$		67.84	31	120	32	4.5[b]		845[d]	21 and 32	0.95	31
Pyrope	$Mg_3Al_2Si_3O_{12}$	Py	113.19		173	33	3.8	34	981	35 and 36	1.24	35 and 36
Almandine	$Fe_3Al_2Si_3O_{12}$		115.23		177	37	4.0[e]		909[f]	37	1.06	38
Grossular	$Ca_3Al_2Si_3O_{12}$	Gr	125.30	38	168	37	4.5	39	904	40	1.05	38
Majorite	$Mg_4Si_4O_{12}$	Maj	114.15[g]		151 (173)	41 (42)	4.0[e] (4.9)	(22)	949[f]	37 and 41	1.24[h]	
	$Fe_4Si_4O_{12}$		117.70[g]		146[i] (168)[i]		4.0[e] (4.9)	(22)	820[f,i]	37	1.24[h]	
Ca-majorite	$Ca_4Si_4O_{12}$	Ca-Maj	127.57[g]		135[i] (155)[i]		4.0[e] (4.9)	(22)	850[f,i]	37	1.24[h]	
Perovskite	$MgSiO_3$	Pv	24.46		262.6	43	3.9	43	1017	44 and 45	1.96	44 and 45
	$FeSiO_3$		25.49		262.6[b]	46	3.9[b]	46	749[j,k]	47	1.96[b]	
Al-perovskite	$Mg_{3/4}Al_{1/2}Si_{3/4}O_3$	Al-Pv	24.84	48	258.6[l]		3.9[b]		1010[k,m]	47	1.96[b]	
	$Fe_{3/4}Al_{1/2}Si_{3/4}O_3$		25.87	48	248.3[l]		3.9[b]		833[k,m]	47	1.96[b]	
Ca-perovskite	$CaSiO_3$	Ca-Pv	27.27	49	301.4	49	3.8	49	917[k,m]	47	1.96[b]	
Periclase	MgO	Mw	11.25		160.4	50	4.13	50	777	4 and 40	1.47	4 and 40
Wustite	FeO		12.25		152.3	51	4.92	51	434[n]	50 and 51	1.48	52

References: 1, *Graham and Barsch* [1969]; 2, *Isaak et al.* [1989]; 3, *Olinger* [1977]; 4, *Suzuki* [1975*a*]; 5, *Ashida et al.* [1987]; 6, *Graham et al.* [1988]; 7, *Williams et al.* [1990]; 8, *Suzuki et al.* [1981]; 9, *Watanabe* [1982]; 10, *Sawamoto et al.* [1984]; 11, *Fei et al.* [1992]; 12, *Gwanmesia et al.* [1990]; 13, *Suzuki et al.* [1980]; 14, *Hazen et al.* [1990]; 15, *Weidner et al.* [1984]; 16, *Sawamoto et al.* [1986]; 17, *Rigden et al.* [1991]; 18, *Suzuki* [1979]; 19, *Liebermann* [1975]; 20, *Bass et al.* [1981]; 21, *Weidner et al.* [1978]; 22, *Duffy and Anderson* [1989]; 23, *Watt and Ahrens* [1986]; 24, *Suzuki* [1975*b*]; 25, *Krupka et al.* [1985]; 26, *Bass and Weidner* [1984]; 27, *Sueno et al.* [1976]; 28, *Finger and Ohashi* [1976]; 29, *Levien et al.* [1979]; 30, *Levien and Prewitt* [1981]; 31, *Cameron et al.* [1973]; 32, *Kandelin and Weidner* [1988]; 33, *O'Neill et al.* [1989]; 34, *Leger et al.* [1990]; 35, *Suzuki and Anderson* [1983]; 36, *Robie et al.* [1976]; 37, *Bass* [1989]; 38, *Skinner* [1956]; 39, *Weaver et al.* [1976]; 40, *Krupka et al.* [1979]; 41, *Bass and Kanzaki* [1990]; 42, *Yeganeh-Haeri et al.* [1990]; 43, *Knittle and Jeanloz* [1987]; 44, *Knittle et al.* [1986]; 45, *Ito and Takahashi* [1989]; 46, *Mao et al.* [1991]; 47, *Yeganeh-Haeri et al.* [1989]; 48, *Weng et al.* [1982]; 49, *Mao et al.* [1989]; 50, *Jackson and Niester* [1982]; 51, *Jackson* [1990]; 52, *Touloukian et al.* [1977].

[a] Unless otherwise noted, volumes are from *Jeanloz and Thompson* [1983].
[b] Assumed to be the same as the Mg end-member.
[c] Dependence on Mg/Fe ratio assumed the same as for spinel.
[d] Calculated from equation (20) and the properties of diopside.
[e] Assumed similar to pyrope.
[f] Calculated from equation (20) and the properties of pyrope.
[g] This work; see text.
[h] Assumed to be the same as pyrope.
[i] Bulk and shear moduli calculated from equation (19) and the properties of Mg-majorite.
[j] Effect of Fe on shear modulus assumed the same as for enstatite.
[k] Calculated from equation (20) and the properties of Mg-perovskite.
[l] Calculated from equation (19) and the properties of Mg-perovskite.
[m] Shear modulus calculated from equation (19) and the properties of Mg-perovskite.
[n] Elastic value.

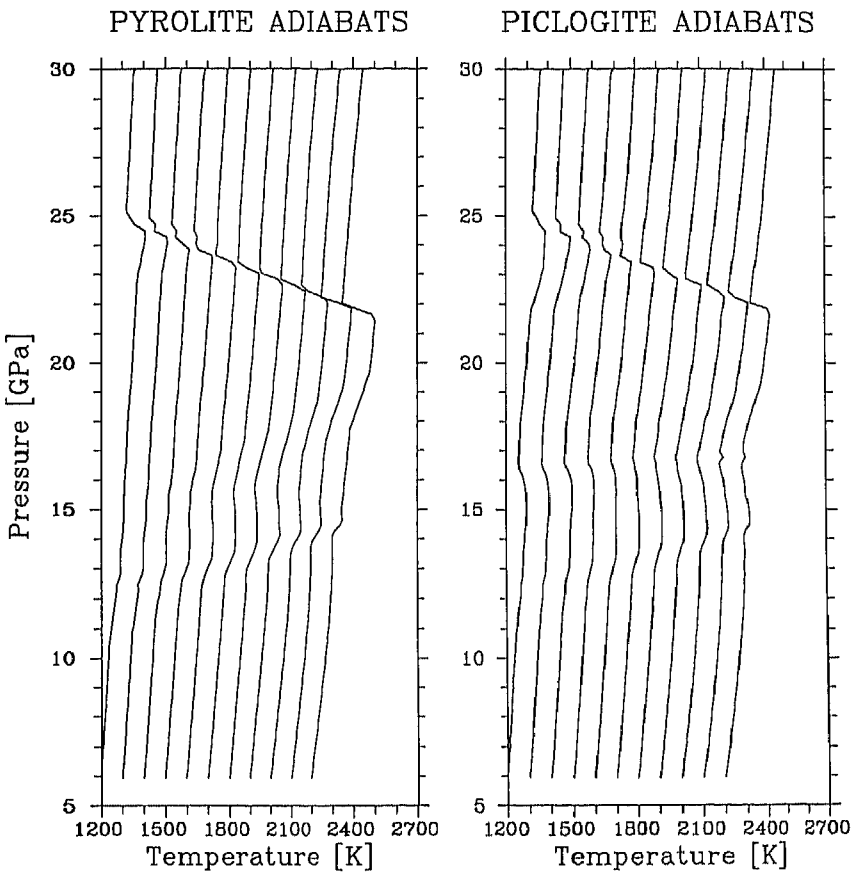

Fig. 3. Isentropes of pyrolite and piclogite compositions.

most minerals are directly measured by X ray diffraction, while those of fictive Fe end-members (Fe-wadsleyite and Fe-perovskite) are determined by measurements along the Mg-Fe join. Using the known volumes of pyrope, almandine, and grossular, we simultaneously inverted diffraction data on a suite of garnets for the molar volumes of Mg, Fe, and Ca majorites. The 30 garnet solid solutions span the range of compositions considered here [*Akaogi and Akimoto*, 1977; *Jeanloz*, 1981; *Irifune et al.*, 1986; *Irifune*, 1987; *Irifune and Ringwood*, 1987*a*]. Derived end-member majorite values are constrained to within 0.1% (68% confidence level) and agree well with previous determinations of Mg and Fe majorite volumes [*Jeanloz*, 1981]. Garnet volumes are explained to within 0.2% by this ideal solution model.

Following the approach of *Bass et al.* [1981], we adopt the directly measured value of K_0, where ultrasonic or brillouin determinations exist, and determine K_0' by inverting compression data. We prefer this approach to determinations of K_0' based on relatively low-pressure ultrasonic measurements of K [e.g., *Gwanmesia et al.*, 1990], since it is based on direct measurement of an observable mantle property (density) at mantle pressure conditions. When experimental constraints are unavailable, we estimate the bulk and shear moduli using velocity-density systematics:

$$M_0 V_0 = M_{0R} V_{0R} \tag{19}$$

where M_0 is the unknown modulus of a mineral, V_0 is its molar volume, and M_{0R} and V_{0R} are the corresponding known properties of a reference mineral (see also, for example, *Duffy and Anderson* [1989]). The K_0 and K_0' of majorites are treated as variable within the range of current estimates and are adjusted to provide the best fit with observed seismic properties. The effect of uncertainties in the thermodynamic parameters is discussed in detail below.

For most minerals, values of θ_0 and γ_0 are constrained by heat capacity and thermal expansivity data as described by *Stixrude and Bukowinski* [1990]. When heat capacity data are not available, we estimate θ_0 by

$$\theta_0/\theta_0^e = \theta_{0R}/\theta_{0R}^e \tag{20}$$

where θ_0 is the unknown thermal Debye temperature of a mineral, θ_0^e is its known elastic Debye temperature, and θ_{0R} and θ_{0R}^e are the corresponding known properties of a reference mineral (see also *Watanabe* [1982]).

RESULTS

Isentropes of pyrolite and piclogite determined from the same thermodynamic potentials used in the mineral elasticity calculations are shown in Figure 3. These isentropes closely approximate geotherms since, for mantle conditions, the effects of viscous dissipation are only significant in narrow boundary layers [*Machetel and Yuen*, 1989]. The calculated geotherms are deflected by the heat of reaction during phase transitions [*Verhoogen*, 1965; *Jeanloz and Thompson*, 1983]. The exothermic nature of phase transitions below 21 GPa causes positive temperature jumps and high gradients in this region compared with the adiabatic

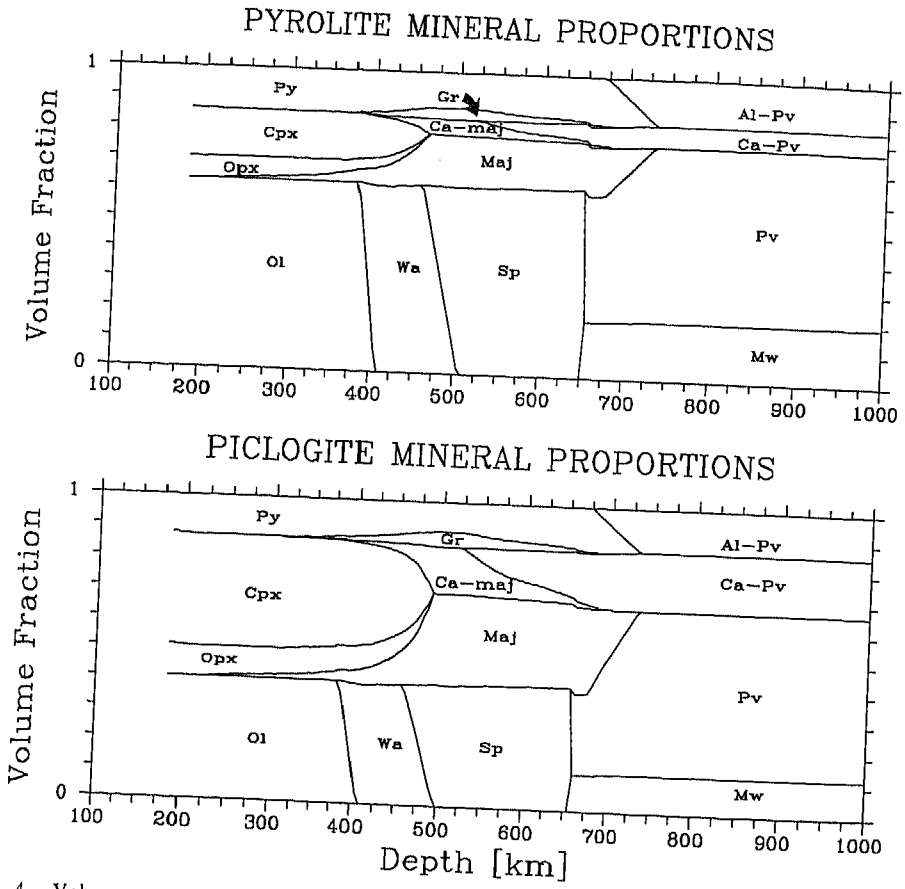

Fig. 4. Volume percentage of the minerals present in piclogite and pyrolite as a function of depth.

compression of individual phases. The transformation of garnet and spinel into perovskite + magnesiowüstite is a strongly endothermic reaction and causes the substantial negative jump seen between pressures of 21 and 25 GPa. Higher pressures induce no further transitions and temperature changes slowly with pressure.

On the basis of our summary phase diagrams (Figures 1 and 2), we estimate relative mineral fractions along a representative mantle adiabat (Figure 4, initial temperature at 185 km depth of 1700°K [*Jeanloz and Morris*, 1986]). Abundances of individual garnet components illustrate their relative effects on the garnet solid solution. The larger bulk Si # (Si # is number of Si atoms per every 12 O atoms) in piclogite is reflected in a reduced olivine content compared with pyrolite. The larger residuum Si # in piclogite causes a larger pyroxene to garnet ratio at low pressures and a larger ratio of majorite to Al-rich garnet components at higher pressures.

Figure 5 compares density profiles of the total assemblage for piclogite and pyrolite with the mean and standard deviation of 14 published Earth models [*Derr*, 1969; *Haddon and Bullen*, 1969; *Mizutani and Abe*, 1971; *Wang*, 1972; *Jordan and Anderson*, 1974; *Gilbert and Dziewonski*, 1975; *Kind and Muller*, 1975; *Hart et al.*, 1976; *Nakada and Hashizume*, 1983; *Lerner-Lam and Jordan*, 1987; *Montagner and Anderson*, 1989; *Dost*, 1990]. Pyrolite agrees very well with the measured profile throughout the entire upper mantle and the upper part of the lower mantle. Piclogite, on the other hand, matches the observed density in the uppermost mantle, the lower part of the transition zone, and the upper part of the lower mantle but departs significantly from observations between 400 and 500 km depth.

Acoustic velocity profiles of the individual minerals present in the two assemblages and their composite value are shown in Figures 6 and 7. Also shown are the mean and standard error of V_Φ in the upper mantle based on 34 P wave velocity (V_P) profiles and 32 S wave velocity (V_S) profiles generated from high-resolution travel time studies or waveform modeling studies of body waves or surface waves [*Chinnery and Toksoz*, 1967; *Herrin*, 1968; *Fairborn*, 1969; *Randall*, 1971; *Buchbinder*, 1971; *Wright and Cleary*, 1972; *Gilbert and Dziewonski*, 1975; *Hart*, 1975; *Kind and Muller*, 1975; *Dey-Sarkar and Wiggins*, 1976; *Hart et al.*, 1976; *King and Calcagnile*, 1976; *Fukao*, 1977; *Burdick and Helmberger*, 1978; *Sengupta and Julian*, 1978; *McMechan*, 1979, 1981; *Uhrhammer*, 1979; *Given and Helmberger*, 1980; *Hales et al.*, 1980; *Burdick*, 1981; *Dziewonski and Anderson*, 1981; *Vinnik and Ryaboy*, 1981; *Fukao et al.*, 1982; *Nakada and Hashizume*, 1983; *Grand and Helmberger*, 1984*a*, *b*; *Walck*, 1984, 1985; *Lyon-Caen*, 1986; *Lerner-Lam and Jordan*, 1987; *Paulssen*, 1987; *Grad*, 1988; *Graves and Helmberger*, 1988; *Montagner and Anderson*, 1989; *Lefevre and Helmberger*, 1989; *Bowman and Kennett*, 1990; *Dost*, 1990; *Kennett and Engdahl*, 1991]. These properties were derived using the mean and standard deviation of V_P and V_S in standard statistical formulae [see *Bevington*, 1969] and through a Monte Carlo method of generating a distribution of V_Φ utilizing all possible combinations of the V_P and V_S profiles. The results of each approach were nearly identical,

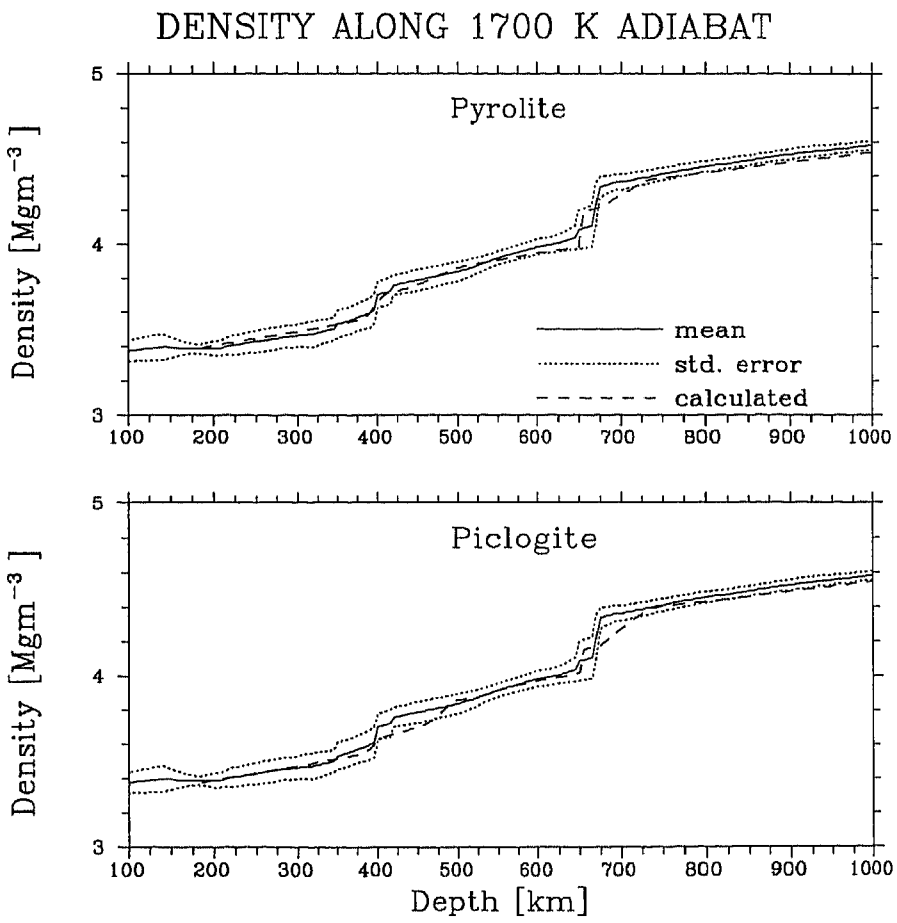

Fig. 5. Bulk density of pyrolite and piclogite as a function of depth. The mean and standard deviation of densities inferred from seismic observations are represented by the solid and dotted lines, respectively.

indicating that the statistical properties of V_Φ reported here are robust.

In the uppermost mantle, both assemblages are equally consistent with the mean velocity profile. Near the 400-km discontinuity, the characters of piclogite and pyrolite differ significantly. The pyrolite model predicts a strong jump in velocity occurring in a relatively narrow depth range followed by a smooth increase in velocity within the transition zone. Piclogite predicts a jump that is only two-thirds of the expected value. The velocity remains consistently low for the next 50 km and then rises to the expected value within a 30-km-depth range. A rise in velocity occurs near the proposed 520-km seismic discontinuity [*Shearer*, 1990] in both assemblages, though it is more pronounced in piclogite. In the upper part of the lower mantle, the velocities predicted by piclogite and pyrolite are consistently higher than those deduced from seismic observations.

Discussion

Both compositions readily account for the anomalously high velocity and density gradients observed in the transition zone. The combination of the pyroxene to garnet transition in the shallow parts of the transition zone, the wadsleyite to spinel transition at intermediate depths, and the appearance of Ca-perovskite at the base of this layer produces velocity and density gradients in pyrolite which are similar to those observed and averaged velocity gradients in piclogite which are 30% larger. These results show that a chemically homogeneous layer can account for the observed properties of the transition zone.

Pyrolite and piclogite are both consistent with observed density and bulk sound velocity profiles above 400 km and below 500 km and with observations of the 400-km discontinuity. In both compositions, the transition to wadsleyite causes rapid increases in velocity over a 20-km interval near 400 km. This is consistent with the depth (390–420 km) and width (10–20 km) of the discontinuity in most seismic models [*Walck*, 1984; *Paulssen*, 1987]. The much sharper gradient found by *Leven* [1985] (less than 6 km wide) may not be representative of the normal mantle because the earthquakes used in this study were located in or near a subduction zone. High thermal gradients present in these areas may tend to sharpen the discontinuity by narrowing the dissolution width of relevant phase changes or give the appearance of a sharp discontinuity by focusing seismic energy at higher frequencies. Pyrolite predicts a 4.5% velocity jump at the discontinuity, in excellent agreement with recent P and S wave velocity profiles, which predict a jump in bulk sound velocity of 4.5–6% (Figure 8) [*Walck*, 1984; *Grand and Helmberger*, 1984*a*; *Leven*, 1985; *Paulssen*, 1987; *Lefevre and Helmberger*, 1989; *Kennett and Engdahl*, 1991]. The lesser olivine content in piclogite causes a much smaller velocity jump

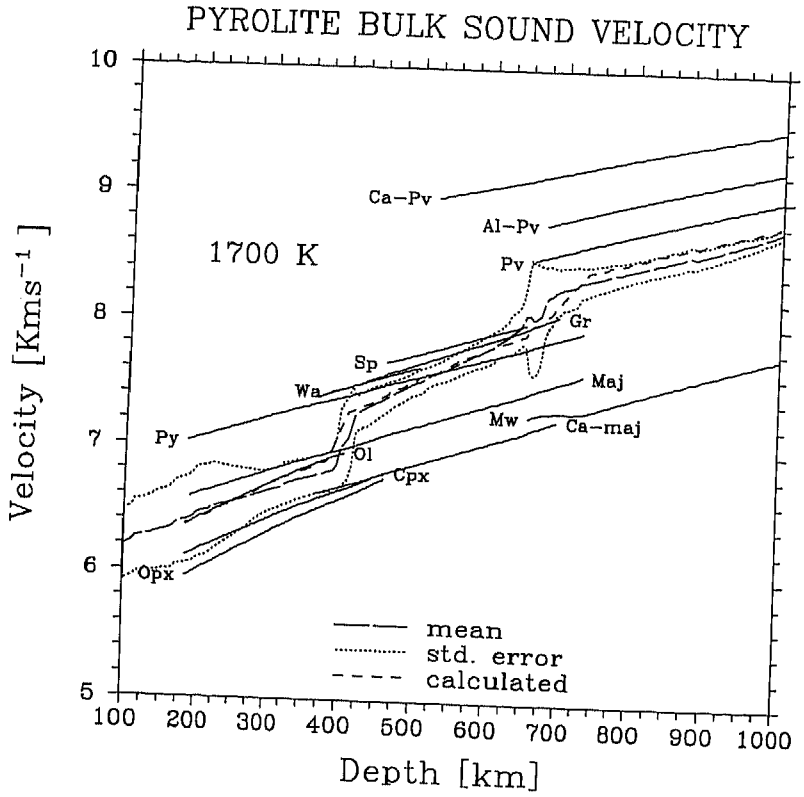

Fig. 6. Acoustic velocity of individual phases (solid lines) and the composite velocity of pyrolite (short dashed line). The mean and standard deviation of bulk sound velocity calculated from various seismic studies are represented by the long dashed and dotted lines, respectively.

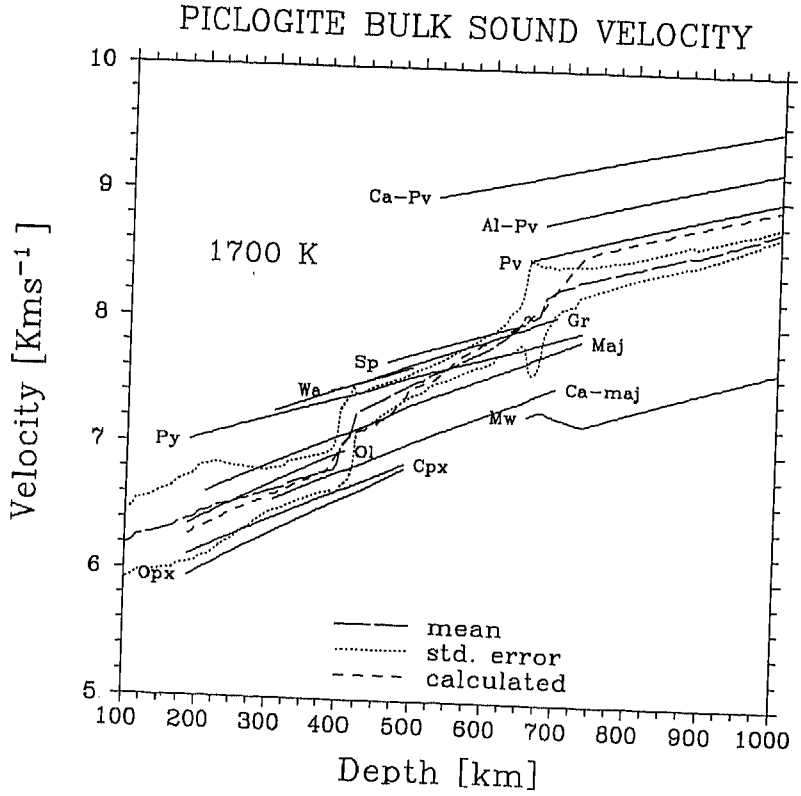

Fig. 7. Same as Figure 6 for the piclogite composition.

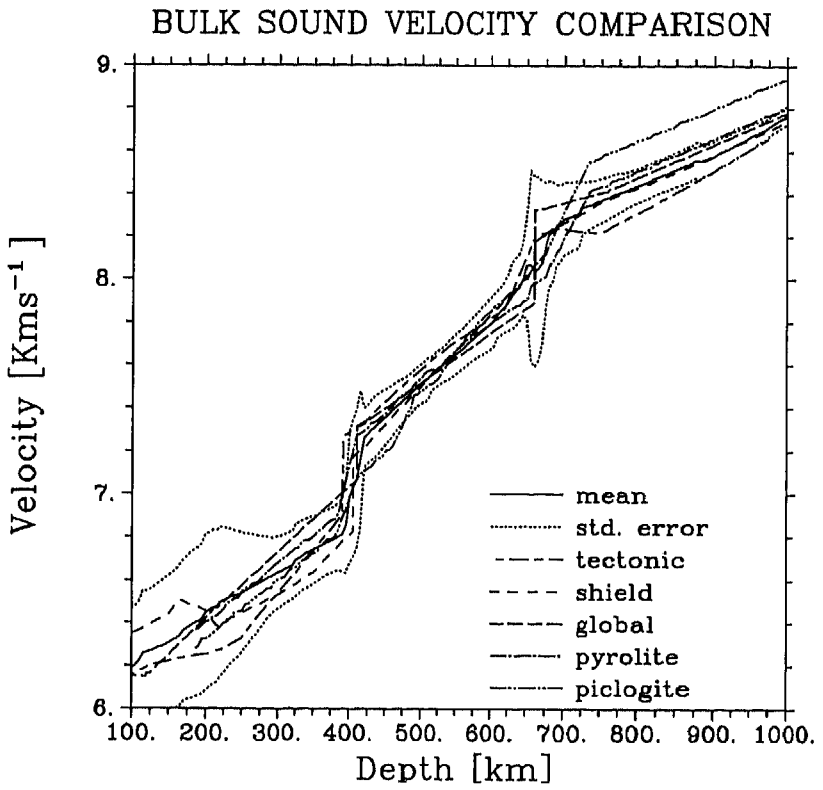

Fig. 8. Composite bulk sound velocity V_Φ of piclogite and pyrolite compared to individual curves observed in Earth. The tectonic profile representative of tectonically active regions is calculated from the *P* wave profile of *Walck* [1984] and the tectonic *S* wave profile of *Grand and Helmberger* [1984*a*]. The shield profile representative of cratonic regions is calculated from the *P* wave model of *Lefevre and Helmberger* [1989] and the shield *S* wave model of *Grand and Helmberger* [1984*a*]. The global model is calculated from the average *P* and *S* wave models of *Kennett and Engdahl* [1991].

(3.3%) which is nevertheless marginally consistent with observed conversions at the discontinuity [*Bock and Kind*, 1991].

Of the two compositions, we find that only pyrolite agrees with observations throughout the upper mantle and transition zone, in excellent agreement with the results of *Weidner* [1985] and *Weidner and Ito* [1987]. Just below the 400-km discontinuity, piclogite deviates significantly from the data. The smaller amount of Al in piclogite delays the pyroxene to garnet transition to higher pressures (Figure 4), causing anomalously low velocities and densities extending 80 km below the discontinuity.

We illustrate the effect of uncertainties in the thermodynamic parameters by considering alternative estimates of K and K' of the majorite species and K'_0 of wadsleyite and spinel species (Table 3). Variation of other parameters within their uncertainties has a comparatively small effect on derived mantle velocities. For pyrolite, values of K of majorites and K'_0 of majorites, wadsleyite, and spinel at the lower extreme of current estimates were used to generate Figures 5 and 6. Higher majorite bulk moduli lead to higher bulk sound velocities in the transition zone, causing pyrolite to deviate significantly from the observed profile (Figure 9). Although raising mantle temperatures can reconcile calculated velocities with observation, higher temperatures lead to disagreement with observed densities. Adopting high values of K'_0 for wadsleyite does not affect the acceptability of pyrolite, although high values of K'_0 for spinel cause significant disagreement just above the 670-km discontinuity. Pyrolite provides an acceptable fit to upper mantle and transition zone properties for values of majorite bulk moduli and spinel K'_0 in the lower half of the range considered here.

Average values of majorite bulk moduli and values of K'_0 of majorite, wadsleyite, and spinel at the lower extreme of current estimates were used to generate Figures 5 and 7. Lower and higher majorite bulk moduli lower and raise transition zone velocities, respectively, and magnify the disparity between piclogite and observed bulk sound velocity profiles. Again, agreement with velocities can be improved by raising or lowering assumed mantle temperatures but only at the expense of the density comparison. Alternative values of K'_0 of wadsleyite and spinel improve agreement with the bulk sound velocity profile but magnify the discrepancy in density between 400 and 500 km (Figure 10). Regardless of variations in the thermodynamic parameters or temperature, piclogite does not provide an acceptable fit to both bulk sound velocity and density profiles.

Pyrolite offers an excellent explanation of the seismic data but not a unique one. We have found modifications of piclogite-type (olivine poor) compositions which are also acceptable. Piclogite can be reconciled with seismic observations by substantially enriching it in Al at the expense of Si. This lowers the pressure of the pyroxene to garnet dissolution, raising velocities immediately below the 400-km discontinuity. The composition shown in Table 4 provides an acceptable fit to observed velocity and density profiles along

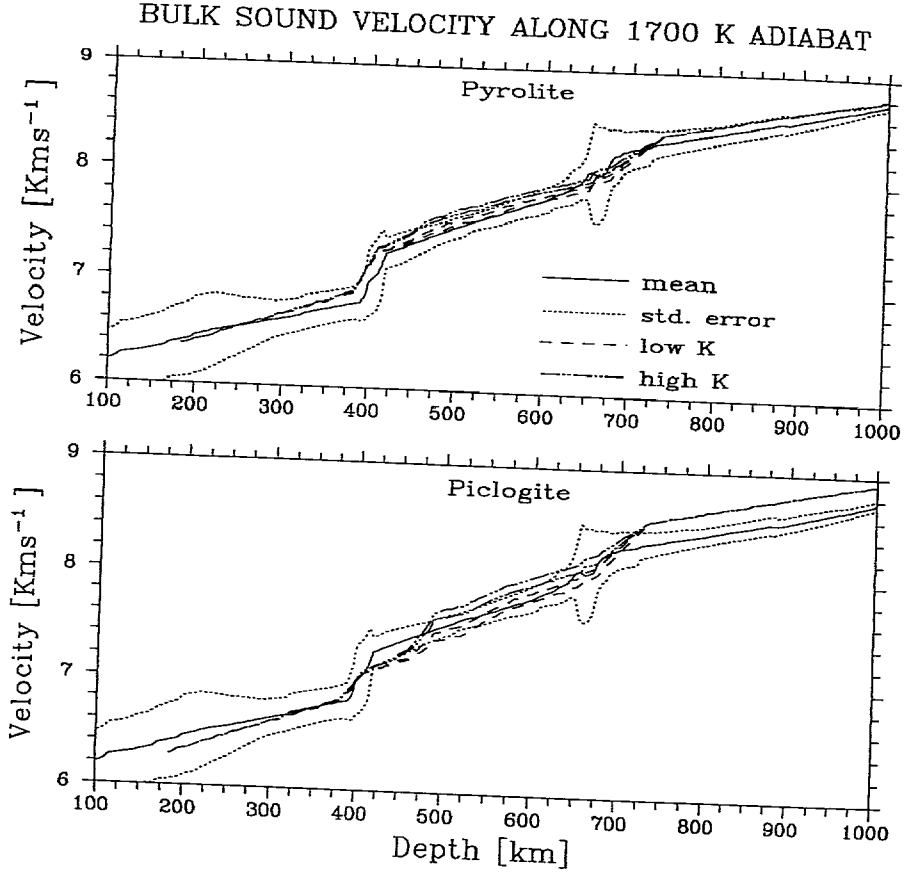

Fig. 9. Effect of the uncertainty in the majorite elastic parameters on the composite profile. High and low values of K produce the higher and lower pairs of dashed curves, respectively. High and low values of K' produce the higher and lower curves for each pair. The mean and standard deviation of observed velocities are represented by the solid and dotted lines, respectively.

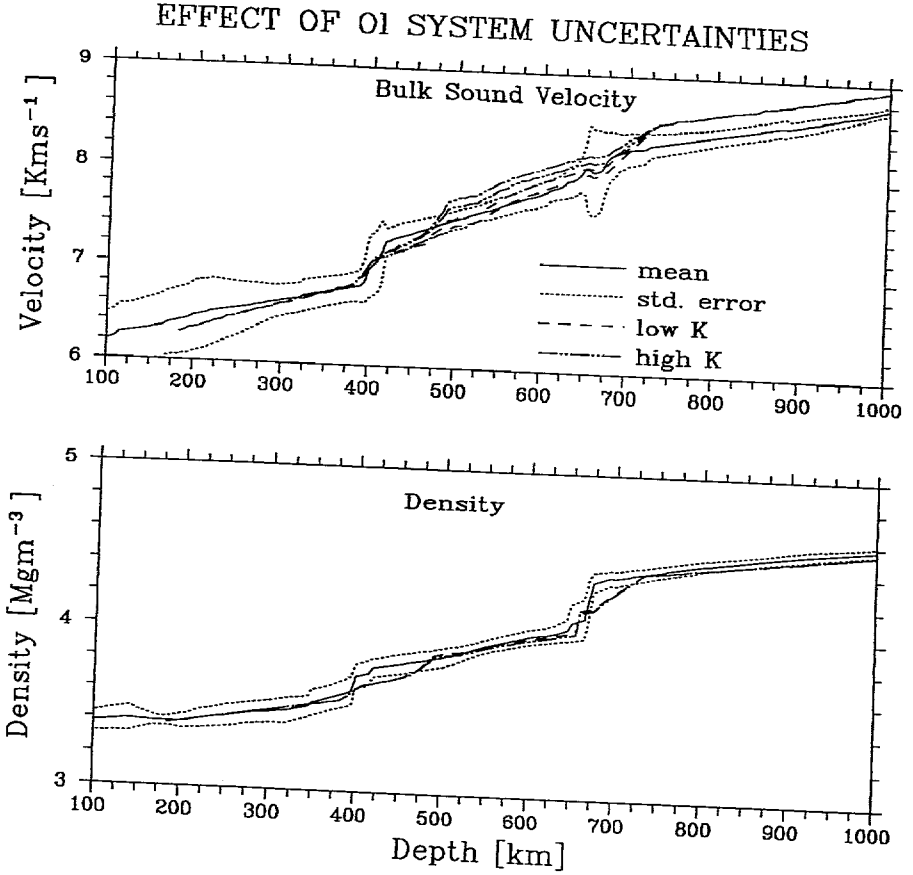

Fig. 10. Effect of the uncertainty in the majorite elastic parameters coupled with a K' value of 4.8 and 5.0 for wadsleyite and spinel, respectively, on the bulk sound velocity and density of piclogite. High and low values of majorite bulk moduli produce the higher and lower pairs of dashed curves, respectively. High and low values of K' produce the higher and lower curves for each pair. The mean and standard deviation of observed velocities and densities are represented by the solid and dotted lines, respectively.

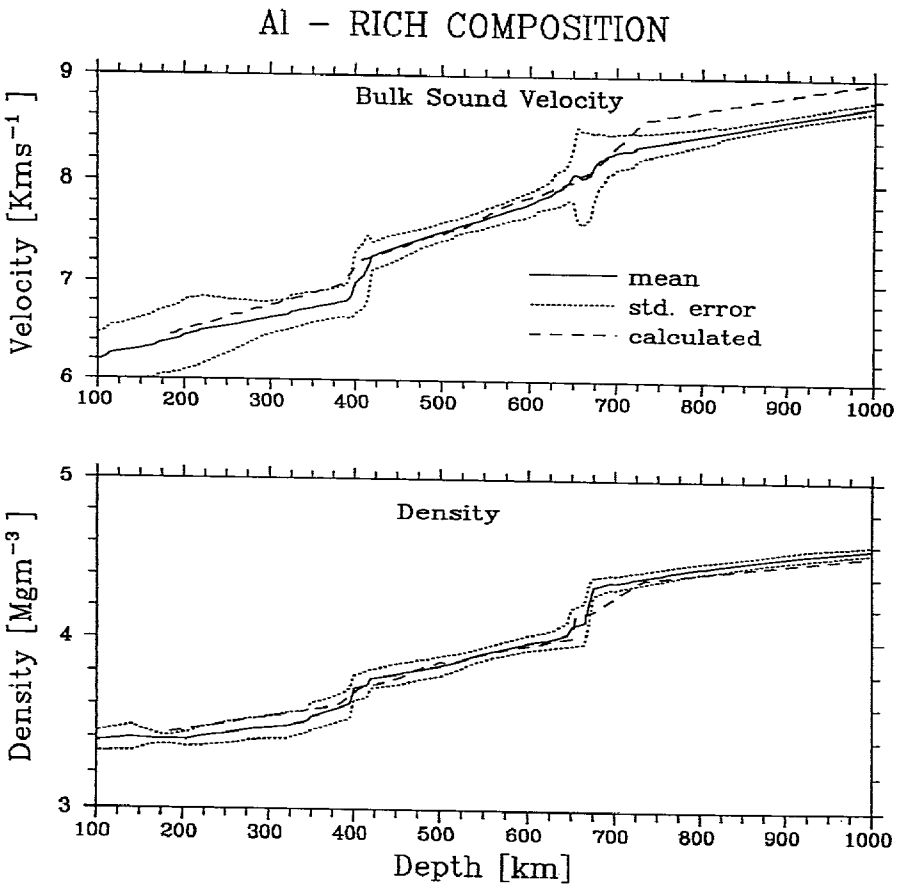

Fig. 11. Composite bulk sound velocity and density curves for an aluminum enriched piclogite. The mean and standard deviation of observed velocities and densities are represented by the solid and dotted lines, respectively.

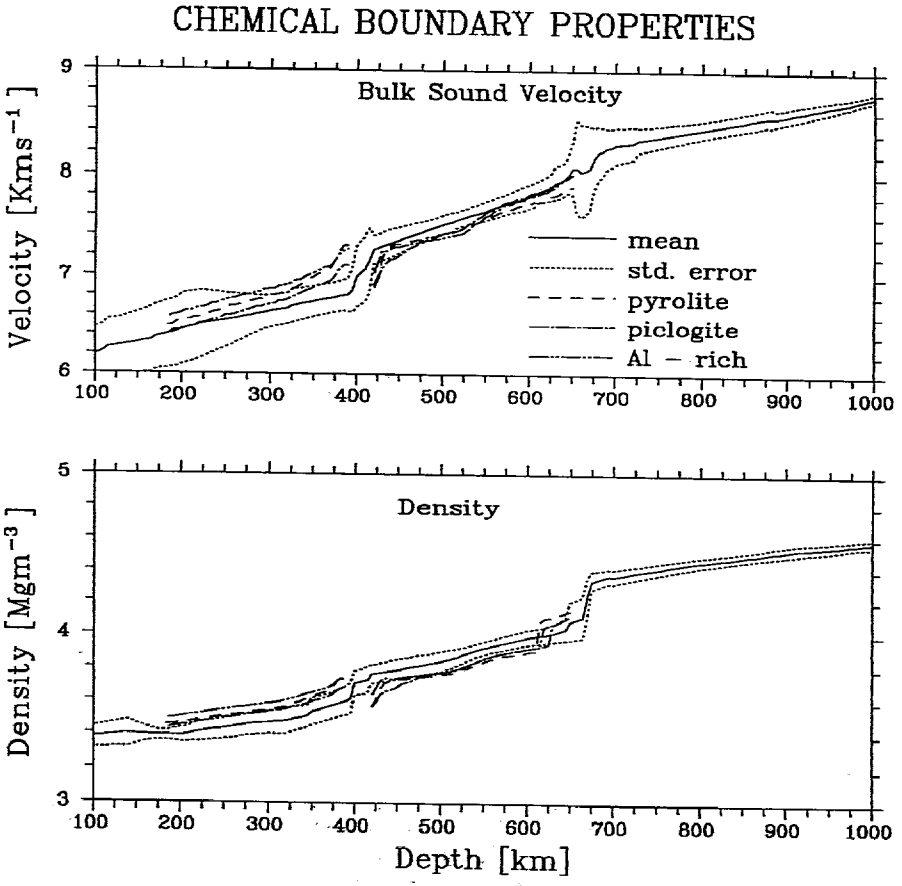

Fig. 12. Effect of a thermal boundary layer on calculated mantle properties. For the three compositions considered here, upper mantle properties are shown along the 1200°K adiabat. Transition zone properties are shown along the 2200°K adiabat. The mean and standard deviation of acoustic velocity and density are represented by the solid and dotted lines (see text for discussion).

TABLE 4. Al-Rich Residuum Composition

	Whole, mol %	Residuum, mol %
SiO_2	39.82	44.81
MgO	42.77	29.50
FeO	5.35	4.34
Al_2O_3	3.30	5.84
CaO	8.76	15.50
Si #	3.26	3.43

the 1700°K adiabat (Figure 11). Recently discovered kimberlite xenoliths, thought to have originated near 400 km depth, also suggest Al-rich compositions [*Sautter et al.*, 1991], although these may not be representative of the bulk transition zone. Sodium enrichment also lowers the pyroxene to garnet transition and may also improve agreement with a piclogite-type composition [*Gasparik*, 1990].

For the range of compositions considered here, a chemically layered upper mantle is unlikely. Adiabats initiating at 1700°–1800°K at 185 km lead to the best agreement with observed transition zone properties regardless of composition. These temperatures agree very well with independent determinations from geothermometry [see *Jeanloz and Knittle*, 1989]. A chemical boundary at 400 km, however, requires layered convection and a thermal boundary at this depth of 500°–1000°K [*Jeanloz and Richter*, 1979]. Retaining a 1700°K adiabat in the uppermost mantle, we find that transition zone properties along a 2200°K adiabat are in severe disagreement with observed densities (Figure 12). Furthermore, these high temperatures may cause wide spread partial melting of the transition zone (Figures 1 and 2), leading to shear velocities much lower than observed. Alternatively, if we assume a 1700°K adiabat in the transition zone, the uppermost mantle follows a 1200°K adiabat which is marginally consistent with seismic data for some compositions (Figure 12) but inconsistent with geothermometry.

Our results indicate that the upper mantle, while probably not internally layered, is chemically distinct from the lower mantle. In agreement with many previous studies, we find that the MgO-FeO-SiO_2 fraction of the compositions considered here are marginally consistent with observed lower mantle properties [e.g., *Jackson*, 1983; *Bukowinski and Wolf*, 1990]. However, consideration of the CaO component degrades the comparison. Through Ca-perovskite, likely the fastest mantle mineral (highest bulk sound velocity, Figures 6 and 7), the CaO component causes complete pyrolite, piclogite, and Al-rich piclogite to overestimate bulk sound velocities at the top of the lower mantle by 1, 2, and 3%, respectively, the larger differences for the latter two reflecting their greater CaO content. Lower mantle densities are also underestimated by all three models. Propagation of uncertainties in the thermodynamic parameters shows that these discrepancies are significant and that all three compositions can be rejected at the 68% confidence level as acceptable models of the lower mantle [*Stixrude and Ita*, 1991]. By considering the effects of Ca-perovskite, our results considerably strengthen those of previous studies which suggested that compositions different from pyrolite best match the lower mantle [e.g., *Jeanloz and Knittle*, 1989; *Bina and Silver*, 1990]. Furthermore, Ca-perovskite may provide an explanation of the proposed 520-km seismic discontinuity [*Shearer*, 1990]. The transformation of garnet to Ca-perovskite near 18 GPa produces anomalous velocity gradients in all the compositions considered here which may account for the observed reflections (Figures 6 and 7).

CONCLUSIONS

Self-consistent temperature, density, and velocity profiles show that pyrolite agrees very well with seismic observations throughout the upper mantle and transition zone. Piclogite significantly underestimates velocities and densities between 400 and 500 km. Substantially enriching piclogite in Al, though, produces an acceptable fit to seismic data at all depths. Thus seismic and mineral physics data are able to reject some models, but they cannot uniquely determine the composition of the transition zone given their present precision. Consideration of shear wave velocities may further limit the range of acceptable compositions. The lack of laboratory measurements of shear moduli under mantle pressure conditions currently limits this approach. Our results indicate that chemical layering of the upper mantle is unlikely. Thus petrologic constraints on the composition of the uppermost mantle can be combined with seismic and mineral physics data to determine transition zone composition.

All the compositions considered here show anomalous velocity gradients near 18 GPa due to the transformation of garnet to Ca-perovskite. This transformation may explain the proposed 520 km seismic discontinuity. The high bulk sound velocity of Ca-perovskite causes overestimated velocities in the upper part of the lower mantle for all compositions, implying a change in composition at 660 km and layered convection in the Earth.

Acknowledgments. We thank M. Akaogi and an anonymous referee for their constructive reviews and C. Lithgow-Bertelloni, M. S. T. Bukowinski, G. Helffrich, R. Jeanloz and L. Johnson for comments which improved the manuscript. We are also grateful to M. S. T. Bukowinski and L. Johnson for many enlightening discussions. This research was supported by grants EAR-8720879 and EAR-9105515 of the National Science Foundation and by the Director, Office of Energy Research, Division of Basic Energy Sciences, Engineering, and Geosciences, of the U.S. Department of Energy under contract DE-AC03-76SF0098. All computations were carried out at the Center for Computational Seismology of the Lawrence Berkeley Laboratory.

REFERENCES

Akaogi, M., and S. Akimoto, Pyroxene-garnet solid-solution equilibria in the systems $Mg_4Si_4O_{12}$-$Mg_3Al_2Si_3O_{12}$ and $Fe_4Si_4O_{12}$-$Fe_3Al_2Si_3O_{12}$ at high pressures and temperatures, *Phys. Earth Planet. Inter.*, *15*, 90–106, 1977.

Akaogi, M., and S. Akimoto, High-Pressure phase equilibria in a garnet lherzolite, with special reference to Mg^{2+}-Fe^{2+} partitioning among constituent minerals, *Phys. Earth Planet. Inter.*, *19*, 31–51, 1979.

Akaogi, M., A. Navrotsky, T. Yagi, and S. Akimoto, Pyroxene-garnet transformation: Thermochemistry and elasticity of garnet solid solutions and application to a pyrolite mantle, in *High-Pressure Research in Mineral Physics*, *Geophys. Monogr. Ser.*, vol. 39, edited by M. H. Manghnani and Y. Syono, pp. 251–260, AGU, Washington, D. C., 1987.

Akaogi, M., E. Ito, and A. Navrotsky, Olivine-modified spinel-spinel transitions in the system Mg_2SiO_4-Fe_2SiO_4: Calorimetric measurements, Thermochemical calculation, and geophysical application, *J. Geophys. Res.*, *94*, 15,671–15,685, 1989.

Allègre, C. J., and D. L. Turcotte, Geodynamic mixing in the

mesosphere boundary layer and the origin of oceanic islands, *Geophys. Res. Lett.*, *12*, 207–210, 1985.

Anderson, D. L., and J. D. Bass, Mineralogy and composition of the upper mantle, *Geophys. Res. Lett.*, *11*, 637–640, 1984.

Anderson, D. L., and J. D. Bass, Transition region of the Earth's upper mantle, *Nature*, *320*, 321–328, 1986.

Ashida, T., S. Kume, and E. Ito, Thermodynamic aspects of phase boundary among α-, β-, and γ-Mg_2SiO_4, in *High-Pressure Research in Mineral Physics*, *Geophys. Monogr. Ser.*, vol. 39, edited by M. H. Manghnani and Y. Syono, pp. 269–274, AGU, Washington, D. C., 1987.

Bass, J. D., Elasticity of grossular and spessartite garnets by Brillouin spectroscopy, *J. Geophys. Res.*, *94*, 7621–7628, 1989.

Bass, J. D., and M. Kanzaki, Elasticity of a majorite-pyrope solid solution, *Geophys. Res. Lett.*, *17*, 1989–1992, 1990.

Bass, J. D., and D. J. Weidner, Elasticity of single-crystal orthoferrosilite, *J. Geophys. Res.*, *89*, 4359–4371, 1984.

Bass, J. D., R. C. Liebermann, D. J. Weidner, and S. J. Finch, Elastic Properties from acoustic and volume compression experiments, *Phys. Earth Planet. Inter.*, *25*, 140–158, 1981.

Bevington, P. R., *Data Reduction and Error Analysis for the Physical Sciences*, 336 pp., McGraw-Hill, New York, 1969.

Bina, C. R., and P. G. Silver, Constraints on lower mantle composition and temperature from density and bulk sound velocity profiles, *Geophys. Res. Lett.*, *17*, 1153–1156, 1990.

Bina, C. R., and B. J. Wood, Olivine-Spinel transitions: Experimental and thermodynamic constraints and implications for the nature of the 400-km seismic discontinuity, *J. Geophys. Res.*, *92*, 4853–4866, 1987.

Birch, F., Elasticity and constitution of the Earth's interior, *J. Geophys. Res.*, *57*, 227–286, 1952.

Bock, G., and R. Kind, A global survey of *S* to *P* and *P* to *S* conversions in the upper mantle transition zone, *Geophys. J. Int.*, *107*, 117–129, 1991.

Bowman, J. R., and B. L. N. Kennett, An investigation of the upper mantle beneath NW Australia using a hybrid seismograph array, *Geophys. J. Int.*, *101*, 411–424, 1990.

Buchbinder, G. G. R., A velocity structure of the Earth's core, *Bull. Seismol. Soc. Am.*, *61*, 429–456, 1971.

Bukowinski, M. S. T., and G. H. Wolf, Thermodynamically consistent decompression: Implications for lower mantle composition, *J. Geophys. Res.*, *95*, 12,583–12,593, 1990.

Burdick, L. J., A comparison of the upper mantle structure beneath North America and Europe, *J. Geophys. Res.*, *86*, 5926–5936, 1981.

Burdick, L. J., and D. V. Helmberger, The upper mantle *P* velocity structure of the western United States, *J. Geophys. Res.*, *83*, 1699–1712, 1978.

Callen, H. B., *Thermodynamics and an Introduction to Thermostatistics*, 493 pp., John Wiley, New York, 1985.

Cameron, M., S. Sueno, C. T. Prewitt, and J. J. Papike, High-temperature crystal chemistry of acmite, diopside, hedenbergite, jadeite, spodumene, and ureyite, *Am. Mineral.*, *58*, 594–618, 1973.

Chinnery, M. A., and M. N. Toksoz, *P*-wave velocities in the mantle below 700 km, *Bull. Seismol. Soc. Am.*, *57*, 199–226, 1967.

Creager, K. C., and T. H. Jordan, Slab penetration into the lower mantle, *J. Geophys. Res.*, *89*, 3031–3049, 1984.

Creager, K. C., and T. H. Jordan, Slab penetration into the lower mantle beneath the Mariana and other island arcs of the northwest Pacific, *J. Geophys. Res.*, *91*, 3573–3589, 1986.

Davies, G. F., Geophysical and isotopic constraints on mantle convection: An interim synthesis, *J. Geophys. Res.*, *89*, 6017–6040, 1984.

DePaolo, D. J., Geochemical evolution of the crust and mantle, *Rev. Geophys.*, *21*, 1347–1358, 1983.

Derr, J. S., Internal structure of the Earth inferred from free oscillations, *J. Geophys. Res.*, *74*, 5202–5220, 1969.

Dey-Sarkar, S. K., and R. A. Wiggins, Upper mantle structure in western Canada, *J. Geophys. Res.*, *81*, 3619–3632, 1976.

Dost, B., Upper mantle structure under western Europe from fundamental and higher mode surface waves using the NARS array, *Geophys. J. Int.*, *100*, 131–151, 1990.

Duffy, T. S., and D. L. Anderson, Seismic velocities in mantle minerals and the mineralogy of the upper mantle, *J. Geophys. Res.*, *94*, 1895–1912, 1989.

Dziewonski, A. M., and D. L. Anderson, Preliminary reference Earth model, *Phys. Earth Planet. Inter.*, *25*, 297–356, 1981.

Fairborn, J. W., Shear wave velocities in the lower mantle, *Bull. Seismol. Soc. Am.*, *59*, 1983–1999, 1969.

Fei, Y., H. Mao, and B. O. Mysen, Experimental determination of element partitioning and calculation of phase relations in the MgO-FeO-SiO_2 system at high pressure and high temperature, *J. Geophys. Res.*, *96*, 2157–2170, 1991.

Fei, Y., H. Mao, J. Shu, G. Parthasarathy, W. Bassett, and J. K., Simultaneous high P-T X ray diffraction study of β-$(Mg,Fe)_2SiO_4$ to 26 GPa and 900 K, *J. Geophys. Res.*, *97*, 4489–4495, 1992.

Finger, L. W., and Y. Ohashi, The thermal expansion of diopside to 800°C and a refinement of the crystal structure at 700°C, *Am. Mineral.*, *61*, 303–310, 1976.

Fukao, Y., Upper mantle *P* structure on the ocean side of the Japan-Kurile arc, *Geophys. J. R. Astron. Soc.*, *50*, 621–642, 1977.

Fukao, Y., T. Nagahashi, and S. Mori, Shear velocity in the mantle transition zone, in *High Pressure Research in Geophysics*, by S. Akimoto and M. H. Manghnani, pp. 285–300, Center for Academic Publications, Tokyo, 1982.

Gasparik, T., Phase relations in the transition zone, *J. Geophys. Res.*, *95*, 15,751–17,769, 1990.

Giardini, D., and J. H. Woodhouse, Deep seismicity and modes of deformation in Tonga subduction zone, *Nature*, *307*, 505–509, 1984.

Gilbert, F., and A. M. Dziewonski, An application of normal mode theory to the retrieval of structural parameters and source mechanisms from seismic spectra, *Philos. Trans. R. Soc. London, Ser. A*, *278*, 187–269, 1975.

Given, J. W., and D. V. Helmberger, Upper mantle structure of northwestern Eurasia, *J. Geophys. Res.*, *85*, 7183–7194, 1980.

Grad, M., Seismic model of the Earth's crust and upper mantle for the east European platform, *Phys. Earth Planet. Inter.*, *51*, 182–184, 1988.

Graham, E., and G. Barsch, Elastic constants of single-crystal forsterite as a function of temperature and pressure, *J. Geophys. Res.*, *74*, 5949–5960, 1969.

Graham, E., J. Schwab, S. Sopkin, and H. Takei, The pressure and temperature dependence of the elastic properties of single-crystal fayalite Fe_2SiO_4, *Phys. Chem. Miner.*, *16*, 186–198, 1988.

Grand, S. P., and D. V. Helmberger, Upper mantle shear structure of North America, *Geophys. J. R. Astron. Soc.*, *76*, 399–438, 1984*a*.

Grand, S. T., and D. V. Helmberger, Upper mantle shear structure beneath the northwest Atlantic Ocean, *J. Geophys. Res.*, *89*, 11,465–11,475, 1984*b*.

Graves, R. W., and D. V. Helmberger, Upper mantle cross section from Tonga to Newfoundland, *J. Geophys. Res.*, *93*, 4701–4711, 1988.

Guggenheim, E. A., *Mixtures*, 270 pp., Clarendon, Oxford, 1952.

Gurnis, M., and G. F. Davies, Mixing in numerical models of mantle convection incorporating plate kinematics, *J. Geophys. Res.*, *91*, 6375–6395, 1986.

Gwanmesia, G., S. Rigden, I. Jackson, and R. Liebermann, Pressure dependence of elastic wave velocity for β-Mg_2SiO_4 and the composition of the Earth's mantle, *Science*, *250*, 794–797, 1990.

Haddon, R. A. W., and K. E. Bullen, An Earth model incorporating free oscillation data, *Phys. Earth Planet. Inter.*, *2*, 35–49, 1969.

Hager, B. H., and M. A. Richards, Long-wavelength variations in Earth's geoid: Physical models and dynamical implications, *Philos. Trans. R. Soc. London, Ser. A*, *328*, 309–327, 1989.

Hales, A. L., K. J. Muirhead, and J. M. W. Rynn, A compressional velocity distribution for the upper mantle, *Tectonophysics*, *63*, 309–348, 1980.

Hardy, R. J., Temperature and pressure dependence of intrinsic anharmonic and quantum corrections to the equation of state, *J. Geophys. Res.*, *85*, 7011–7015, 1980.

Hart, R. S., Shear velocity in the lower mantle from explosion data, *J. Geophys. Res.*, *80*, 4889–4894, 1975.

Hart, R. S., D. L. Anderson, and H. Kanamori, Shear velocity and density of an attenuating Earth, *Earth Planet. Sci. Let.*, *32*, 25–34, 1976.

Haselton, H. T., and R. C. Newton, Thermodynamics of pyrope-grossular garnets and their stabilities at high temperatures and high pressures, *J. Geophys. Res.*, *85*, 6973–6982, 1980.

Hashin, Z., and S. Shtrikman, A variational approach to the elastic

behavior of multiphase materials, *J. Mech. Phys. Solids*, *11*, 127–140, 1963.

Hazen, R. M., J. Zhang, and J. Ko, Effects of Fe/Mg on the compressibility of synthetic wadsleyite: β-$(Mg_{1-x}Fe_x)SiO_4$ ($x < 0.25$), *Phys. Chem. Miner.*, *17*, 416–419, 1990.

Herrin, E., 1968 seismological tables for *P* phases, *Bull. Seismol. Soc. Am.*, *58*, 1193–1242, 1968.

Irifune, T., An experimental investigation of the pyroxene-garnet transformation in a pyrolite composition and its bearing on the constitution of the mantle, *Phys. Earth Planet. Inter.*, *45*, 324–336, 1987.

Irifune, T., and A. E. Ringwood, Phase transformations in a harzburgite composition to 26 GPa: Implications for dynamical behaviour of the subducting slab, *Earth Planet. Sci. Lett.*, *86*, 365–376, 1987*a*.

Irifune, T., and A. E. Ringwood, Phase transformations in primitive MORB and pyrolite compositions to 25 GPa and some geophysical implications, in *High-Pressure Research in Mineral Physics*, *Geophys. Monogr. Ser.*, vol. 39, edited by M. H. Manghnani and Y. Syono, pp. 231–242, Washington, D. C., 1987*b*.

Irifune, T., T. Sekine, A. E. Ringwood, and W. O. Hibberson, The eclogite-garnetite transformation at high pressure and some geophysical implications, *Earth Planet. Sci. Lett.*, *77*, 245–256, 1986.

Irifune, T., J. Susaki, T. Yagi, and H. Sawamoto, Phase transformations in diopside $CaMgSi_2O_6$ at pressures up to 25 GPa, *Geophys. Res. Lett.*, *16*, 187–190, 1989.

Isaak, D. G., O. Anderson, and T. Goto, Elasticity of single-crystal forsterite measured to 1700°K, *J. Geophys. Res.*, *94*, 5895–5906, 1989.

Isacks, B. L., and P. Molnar, Distribution of stresses in the descending lithosphere from a global survey of focal mechanism solutions of mantle earthquakes, *Rev. Geophys.*, *9*, 103–174, 1971.

Ito, E., and E. Takahashi, Ultrahigh-pressure phase transformations and the constitution of the deep mantle, in *High-Pressure Research in Mineral Physics*, *Geophys. Monogr. Ser.*, vol. 39, edited by M. H. Manghnani and Y. Syono, pp. 221–230, AGU, Washington, D. C., 1987*a*.

Ito, E., and E. Takahashi, Melting of peridotite at uppermost lower-mantle conditions, *Nature*, *328*, 514–517, 1987*b*.

Ito, E., and E. Takahashi, Postspinel transformations in the system Mg_2SiO_4-Fe_2SiO_4 and some geophysical implications, *J. Geophys. Res.*, *94*, 10,637–10,646, 1989.

Jackson, I., Some geophysical constraints on the chemical composition of the earth's lower mantle, *Earth Planet. Sci. Lett.*, *62*, 91–103, 1983.

Jackson, I., Elasticity and polymorphism of wüstite $Fe_{1-x}O$, *J. Geophys. Res.*, *95*, 21,671–21,685, 1990.

Jackson, I., and H. Niesler, The elasticity of periclase to 3 GPa and some geophysical implications, in *High Pressure Research in Geophysics*, edited by S. Akimoto and M. H. Manghnani, pp. 93–113, Center for Academic Publications, Tokyo, 1982.

Jarrard, R. D., Relations among subduction parameters, *Rev. Geophys.*, *24*, 217–284, 1986.

Jeanloz, R., Shock wave equation of state and finite strain theory, *J. Geophys. Res.*, *94*, 5873–5886, 1989.

Jeanloz, R., Majorite: Vibrational and compressional properties of a high-pressure phase, *J. Geophys. Res.*, *86*, 6171–6179, 1981.

Jeanloz, R., and E. Knittle, Density and composition of the lower mantle, *Philos. Trans. R. Soc. London, Ser. A*, *328*, 377–389, 1989.

Jeanloz, R., and S. Morris, Temperature distribution in the crust and mantle, *Annu. Rev. Earth Planet. Sci.*, *14*, 377–415, 1986.

Jeanloz, R., and F. M. Richter, Convection, composition, and the thermal state of the lower mantle, *J. Geophys. Res.*, *84*, 5497–5504, 1979.

Jeanloz, R., and A. B. Thompson, Phase transitions and mantle discontinuities, *Rev. Geophys.*, *21*, 51–74, 1983.

Jordan, T. H., and D. L. Anderson, Earth structure from free oscillations and travel times, *Geophys. J. R. Astron. Soc.*, *36*, 411–459, 1974.

Kandelin, J., and D. J. Weidner, Elastic properties of hedenbergite, *J. Geophys. Res.*, *94*, 1063–1072, 1988.

Kanzaki, M., Ultrahigh-pressure phase relations in the system $Mg_4Si_4O_{12}$-$Mg_3Al_2Si_3O_{12}$, *Phys. Earth Planet. Inter.*, *49*, 168–175, 1987.

Kato, T., A. E. Ringwood, and T. Irifune, Experimental determination of element partitioning between silicate perovskites, garnets and liquids: Constraints on early differentiation of the mantle, *Earth Planet. Sci. Lett.*, *89*, 123–145, 1988.

Katsura, T., and E. Ito, The system Mg_2SiO_4-Fe_2SiO_4 at high pressures and temperatures: Precise determination of stabilities of olivine, modified spinel, and spinel, *J. Geophys. Res.*, *94*, 15,663–15,670, 1989.

Kennett, B. L. N., and E. R. Engdahl, Traveltimes for global earthquake location and phase identification, *Geophys. J. Int.*, *105*, 429–465, 1991.

Kim, Y., L. C. Ming, and M. H. Manghnani, A study of phase transformation in hedenbergite to 40 GPa at 1200°C, *Phys. Chem. Miner.*, *16*, 757–762, 1989.

Kind, R., and G. Muller, Computations of *SV* waves in realistic Earth models, *J. Geophys.*, *4*, 149–172, 1975.

King, D. W., and G. Calcagnile, *P*-wave velocities in the upper mantle beneath Fennoscandia and western Russia, *Geophys. J. R. Astron. Soc.*, *46*, 407–432, 1976.

Knittle, E., and R. Jeanloz, Synthesis and equation of state of (Mg, Fe)SiO_3 perovskite to over 100 gigapascals, *Science*, *235*, 666–670, 1987.

Knittle, E., R. Jeanloz, and G. L. Smith, Thermal expansion of silicate perovskite and stratification of the Earth's mantle, *Nature*, *319*, 214–216, 1986.

Knopoff, L., and J. N. Shapiro, Comments on the interrelationships between Grüneisen's parameter and shock and isothermal equations of state, *J. Geophys. Res.*, *74*, 1439–1450, 1969.

Korn, M., P-wave coda analysis of short-period array data and the scattering and absorptive properties of the lithosphere, *Geophys. J. R. Astron. Soc.*, *93*, 437–449, 1988.

Krupka, K. M., R. A. Robie, and B. S. Hemingway, High temperature heat capacities of corundum, periclase, anorthite, $CaAl_2Si_2O_8$ glass, muscovite, pyrophyillite, $KAlSi_3O_8$ glass, grossular, and $NaAlSi_3O_8$ glass, *Am. Mineral.*, *64*, 86–101, 1979.

Krupka, K. M., B. S. Hemingway, R. A. Robie, and D. M. Kerrick, High temperature heat capacities and derived thermodynamic properties of anthophyillite, diopside, dolomite, enstatite, bronzite, talc, tremolite, and wollastonite, *Am. Mineral.*, *70*, 261–271, 1985.

Lefevre, L. V., and D. V. Helmberger, Upper mantle *P* velocity structure of the Canadian shield, *J. Geophys. Res.*, *94*, 17,749–17,765, 1989.

Leger, J. M., A. M. Redon, and C. Chateau, Compressions of synthetic pyrope, spessartine and uvarovite garnets up to 25 GPa, *Phys. Chem. Miner.*, *17*, 161–167, 1990.

Lerner-Lam, A. L., and T. H. Jordan, How thick are the continents?, *J. Geophys. Res.*, *92*, 14,007–14,026, 1987.

Leven, J. H., The application of synthetic seismograms to the interpretation of the upper mantle *P*-wave velocity structure in northern Australia, *Phys. Earth Planet. Inter.*, *38*, 9–27, 1985.

Levien, L. R., and C. T. Prewitt, High pressure structural study of diopside, *Am. Mineral.*, *66*, 315–323, 1981.

Levien, L., D. J. Weidner, and C. T. Prewitt, Elasticity of diopside, *Phys. Chem. Miner.*, *4*, 105–113, 1979.

Liebermann, R. C., Elasticity of olivine (α), beta (β), and spinel (γ) polymorphs of germanates and silicates, *Geophys. J. R. Astron. Soc.*, *42*, 899–929, 1975.

Lyon-Caen, H., Comparison of the upper mantle shear wave velocity structure of the Indian Shield and the Tibetan Plateau and tectonic implications, *Geophys. J. R. Astron. Soc.*, *86*, 727–749, 1986.

Machetel, P., and D. A. Yuen, Penetrative convective flows induced by internal heating and mantle compressibility, *J. Geophys. Res.*, *94*, 10,609–10,626, 1989.

Mao, H. K., L. C. Chen, R. J. Hemley, A. P. Jephcoat, Y. Wu, and W. A. Basset, Stability and equation of state of $CaSiO_3$-perovskite to 134 GPa, *J. Geophys. Res.*, *94*, 17,889–17,894, 1989.

Mao, H. K., R. J. Hemley, Y. Fei, J. F. Shu, L. C. Chen, A. P. Jephcoat, Y. Wu, and W. A. Bassett, Effect of pressure, temperature and composition on lattice parameters and density of (Fe,Mg)SiO_3-perovskites to 30 GPa, *J. Geophys. Res.*, *96*, 8069–8080, 1991.

McMechan, G. A., An amplitude constrained *P*-wave velocity profile for the upper mantle beneath the eastern United States, *Bull. Seismol. Soc. Am.*, *69*, 1733–1744, 1979.

McMechan, G. A., Mantle *P*-wave velocity structure beneath Antarctica, *Bull. Seismol. Soc. Am.*, *71*, 1061–1074, 1981.

McQueen, R. G., S. P. Marsh, J. W. Taylor, J. N. Fritz, and W. J. Carter, The equation of state of solids from shock wave studies, in *High Velocity Impact Phenomena*, edited by R. Kinslow, pp. 294–419, Academic, San Diego, Calif., 1970.

Mizutani, H., and K. Abe, An Earth model consistent with free oscillation and surface wave data, *Phys. Earth Planet. Inter.*, *5*, 345–356, 1971.

Montagner, J., and D. L. Anderson, Constrained reference mantle model, *Phys. Earth Planet. Inter.*, *58*, 205–227, 1989.

Montagner, J. P., and T. Tanimoto, Global upper mantle tomography of seismic velocities and anisotropies, *J. Geophys. Res.*, *96*, 20,337–20,351, 1991.

Nakada, M., and M. Hashizume, Upper mantle structure beneath the Canadian shield derived from higher modes of surface waves, *J. Phys. Earth*, *31*, 387–405, 1983.

Ohashi, Y., and L. Finger, The effect of Ca substitution on the structure of clinoenstatite, *Year Book Carnegie Inst. Washington*, *75*, 743–746, 1976.

Ohashi, Y., C. W. Burnham, and L. Finger, The effect of Ca-Fe substitution on the clinopyroxene crystal structure, *Am. Mineral.*, *60*, 423–434, 1975.

Ohtani, E., Chemical stratification of the mantle formed by melting in the early stage of the terrestrial evolution, *Tectonophysics*, *154*, 201–210, 1988.

Olinger, B., Compression studies of forsterite (Mg_2SiO_4) and enstatite ($MgSiO_3$), in *High-Pressure Research: Applications in Geophysics*, edited by M. H. Manghnani and S. Akimoto, pp. 255–266, Academic, San Diego, Calif., 1977.

O'Neill, B., and R. Jeanloz, Experimental petrology of the lower mantle: A natural peridotite taken to 54 GPa, *Geophys. Res. Lett.*, *17*, 1477–1480, 1990.

O'Neill, B., J. D. Bass, J. R. Smyth, and M. T. Vaughan, Elasticity of grossular-pyrope-almandine garnet, *J. Geophys. Res.*, *94*, 17,819–17,824, 1989.

Paulssen, H., Lateral heterogeneity of Europe's upper mantle as inferred from modelling of broad-band body waves, *Geophys. J. R. Astron. Soc.*, *91*, 171–199, 1987.

Plymate, T. G., and J. H. Stout, A five-parameter temperature corrected Murnaghan equation for P-V-T surfaces, *J. Geophys. Res.*, *94*, 9477–9483, 1989.

Randall, M. J., A revised travel-time table for *S*, *Geophys. J. R. Astron. Soc.*, *22*, 229–234, 1971.

Richet, P., H. Mao, and P. M. Bell, Bulk moduli of magnesiowüstites from static compression measurements, *J. Geophys. Res.*, *94*, 3037–3045, 1989.

Rigden, S. M., G. D. Gwanmesia, J. D. FitzGerald, I. Jackson, and R. C. Liebermann, Spinel elasticity and seismic structure of the transition zone of the mantle, *Nature*, *354*, 143–145, 1991.

Ringwood, A. E., *Composition and Petrology of the Earth's mantle*, 618 pp., McGraw-Hill, New York, 1975.

Robie, R. A., B. S. Hemingway, and J. R. Fisher, Thermodynamic properties of minerals and related substances at 298.15 K and 1 bar (10^5 Pascals) pressure and higher temperatures, *U.S. Geol. Surv. Bull.*, *1452*, 456 pp., 1976.

Salerno, C. M., and J. P. Watt, Walpole bounds on the effective elastic moduli of isotropic multicomponent composites, *J. Appl. Phys.*, *60*, 1618–1624, 1986.

Sautter, V., S. E. Haggerty, and S. Field, Ultradeep (>300 kilometers) ultramafic xenoliths: petrological evidence from the transition zone, *Science*, *252*, 827–830, 1991.

Sawamoto, H., D. Weidner, S. Sasaki, and M. Kumazawa, Single-crystal elastic properties of the modified spinel (beta) phase of Mg_2SiO_4, *Science*, *224*, 749–751, 1984.

Sawamoto, H., M. Kozaki, A. Jujimura, and T. Akamatsu, Precise measurement of compressibility of γ-Mg_2SiO_4 using synchrotron radiation, paper presented at 27th High Pressure Conference, Sapporo, Japan, 1986.

Saxena, S. K., *Thermodynamics of Rock-Forming Minerals*, 188 pp., Springer-Verlag, New York, 1973.

Sengupta, M. K., and B. R. Julian, Radial variation of compressional and shear velocities in the Earth's lower mantle, *Geophys. J. R. Astron. Soc.*, *54*, 185–219, 1978.

Shapiro, J. N., and L. Knopoff, Reduction of shock wave equations of state to isothermal equations of state, *J. Geophys. Res.*, *74*, 1435–1438, 1969.

Shearer, P. M., Seismic imaging of upper-mantle structure with new evidence for a 520-km discontinuity, *Nature*, *344*, 121–126, 1990.

Silver, P. G., and W. W. Chan, Observations of body wave multipathing from broadband seismograms: evidence for lower mantle slab penetration beneath the Sea of Okhotsk, *J. Geophys. Res.*, *91*, 13,787–13,802, 1986.

Silver, P. G., Carlson, R. W., and P. Olson, Deep slabs, geochemical heterogeneity, and the large-scale structure of mantle convection: Investigation of an enduring paradox, *Annu. Rev. Earth Planet. Sci.*, *16*, 477–541, 1988.

Skinner, B. J., Physical properties of end-members of the garnet group, *Am. Mineral.*, *41*, 428–436, 1956.

Stixrude, L., and M. T. Bukowinski, Fundamental thermodynamic relations and silicate melting with implications for the constitution of *D''*, *J. Geophys. Res.*, *95*, 19,311–19,326, 1990.

Stixrude, L., and J. J. Ita, Statistical approach to the determination of lower mantle composition, *Eos Trans. AGU*, *72*, 464, 1991.

Sueno, S., M. Cameron, and C. T. Prewitt, Orthoferrosilite: High temperature crystal chemistry, *Am. Mineral.*, *61*, 38–53, 1976.

Suzuki, I., Thermal expansion of olivine and periclase and their anharmonic properties, *J. Phys. Earth*, *25*, 145–159, 1975*a*.

Suzuki, I., Cell parameters and linear thermal expansion coefficients of orthopyroxenes, *J. Seismol. Soc. Jpn.*, *28*, 1–9, 1975*b*.

Suzuki, I., Thermal expansion of γ-Mg_2SiO_4, *J. Phys. Earth*, *27*, 53–61, 1979.

Suzuki, I., and O. L. Anderson, Elasticity and thermal expansion of a natural garnet up to 1000 K, *J. Phys. Earth*, *31*, 125–138, 1983.

Suzuki, I., E. Ohtani, and M. Kumazawa, Thermal expansion of modified spinel, β-Mg_2SiO_4, *J. Phys. Earth*, *28*, 273–280, 1980.

Suzuki, I., K. Seya, H. Takei, and Y. Sumino, Thermal expansion of fayalite, *Phys. Chem. Miner.*, *7*, 60–63, 1981.

Takahashi, E., and E. Ito, Mineralogy of mantle peridotite along a model geotherm up to 700 km depth, in *High-Pressure Research in Mineral Physics*, *Geophys. Monogr. Ser.*, vol. 39, edited by M. H. Manghnani and Y. Syono, pp. 427–438, AGU, Washington, D. C., 1987.

Tamai, H., and T. Yagi, High-pressure and high-temperature phase relations in $CaSiO_3$ and $CaMgSi_2O_6$ and elasticity of perovskite-type $CaSiO_3$, *Phys. Earth Planet. Inter.*, *54*, 370–377, 1989.

Tonks, W. B., and H. J. Melosh, The physics of crystal settling and suspension in a turbulent magma ocean, in *Origin of the Earth*, edited by H. E. Newsom and J. H. Jones, pp. 151–174, Oxford University Press, New York, 1990.

Touloukian, Y. S., R. S. Kirby, R. E. Taylor, and T. Y. R. Lee, *Thermal Expansion, Nonmetallic Solids*, Plenum, New York, 1977.

Uhrhammer, R., Shear-wave velocity structure for a spherically averaged earth, *Geophys. J. R. Astron. Soc.*, *58*, 749–767, 1979.

Vassiliou, M. S., B. H. Hager, and A. Raefsky, The distribution of earthquakes with depth and stress in subducting slabs, *J. Geodyn.*, *1*, 11–28, 1984.

Verhoogen, J., Phase changes and convection in the Earth's mantle, *Philos. Trans. R. Soc. London, Ser. A*, *258*, 276–283, 1965.

Vinnik, L. P., and V. Z. Ryaboy, Deep structure of the east European platform according to seismic data, *Phys. Earth Planet. Inter.*, *25*, 27–37, 1981.

Walck, M. C., The *P*-wave upper mantle structure beneath an active spreading center: The Gulf of California, *Geophys. J. R. Astron. Soc.*, *76*, 697–723, 1984.

Walck, M. C., The upper mantle beneath the north-east Pacific rim: A comparison with the Gulf of California, *Geophys. J. R. Astron. Soc.*, *81*, 243–276, 1985.

Walker, D., and C. Agee, Partitioning "equilibrium", temperature gradients, and constraints on Earth differentiation, *Earth Planet. Sci. Lett.*, *96*, 49–60, 1989.

Wang, C., A simple Earth model, *J. Geophys. Res.*, *77*, 4318–4329, 1972.

Watanabe, H., Thermochemical properties of synthetic high-pressure compounds relevant to the Earth's mantle, in *High Pressure Research in Geophysics*, edited by S. Akimoto and M. H. Manghnani, pp. 93–113, Center for Academic Publications, Tokyo, 1982.

Watt, J. P., and T. J. Ahrens, Shock wave equation of state of enstatite, *J. Geophys. Res.*, *91*, 7495–7503, 1986.

Watt, J. P., G. F. Davies, and R. J. O'Connell, The elastic properties of composite materials, *Rev. Geophys.*, *14*, 541–563, 1976.

Weaver, J. S., T. Takahashi, and J. Bass, Isothermal compression of grossular garnets to 250 kbars and the effect of calcium on the bulk modulus, *J. Geophys. Res.*, *81*, 2475–2482, 1976.

Weidner, D. J., A mineral physics test of a pyrolite mantle, *Geophys. Res. Lett.*, *12*, 417–420, 1985.

Weidner, D. J., and E. Ito, Mineral physics constraints on a uniform mantle composition, in *High-Pressure Research in Mineral Physics*, *Geophys. Monogr. Ser.*, vol. 39, edited by M. H. Manghnani, and Y. Syono, pp. 439–446, AGU, Washington, D. C., 1987.

Weidner, D. J., H. Wang, and J. Ito, Elasticity of orthoenstatite, *Phys. Earth Planet. Inter.*, *17*, P7–P13, 1978.

Weidner, D. J., H. Sawamoto, and S. Sasaki, Single-crystal elastic properties of the spinel phase of Mg_2SiO_4, *J. Geophys. Res.*, *89*, 7852–7859, 1984.

Weng, K., H. K. Mao, and P. M. Bell, Lattice parameters of the perovskite phase in the system $MgSiO_3$-$CaSiO_3$-Al_2O_3, *Year Book Carnegie Inst. Washington, 1981*, 273–277, 1982.

Williams, Q., E. Knittle, R. Reichlin, S. Martin, and R. Jeanloz, Structural and electronic properties of Fe_2SiO_4-fayalite at ultrahigh pressures: Amorphization and gap closure, *J. Geophys. Res.*, *95*, 21,549–21,564, 1990.

Wood, B. J., Postspinel transformations and the width of the 670-km discontinuity: A comment on "Postspinel transformations in the system Mg_2SiO_4-Fe_2SiO_4 and some geophysical implications", by E. Ito and E. Takahashi, *J. Geophys. Res.*, *95*, 12,681–12,685, 1990.

Wood, B. J., and O. J. Kleppa, Thermochemistry of forsterite-fayalite olivine solutions, *Geochim. Cosmochim. Acta*, *45*, 529–534, 1981.

Wright, C., and J. R. Cleary, *P* wave travel-time gradient measurements for the Warramunga seismic array and lower mantle structure, *Phys. Earth Planet. Inter.*, *5*, 213–230, 1972.

Yeganeh-Haeri, A., D. J. Weidner, and E. Ito, Single crystal elastic moduli of magnesium metasilicate perovskite, in *Perovskite: A Structure of Great Interest to Geophysics and Materials Science*, *Geophys. Monogr. Ser.*, vol. 45, edited by A. Navrotsky and D. J. Weidner, pp. 13–26, AGU, Washington, D. C., 1989.

Yeganeh-Haeri, A., D. J. Weidner, and E. Ito, Elastic properties of the pyrope-majorite solid solution series, *Geophys. Res. Lett.*, *17*, 2453–2456, 1990.

Zhou, H., and R. W. Clayton, *P* and *S* wave travel time inversions for subducting slabs under island arcs of the northwest Pacific, *J. Geophys. Res.*, *95*, 6829–6851, 1990.

Zindler, A., and S. Hart, Chemical geodynamics, *Annu. Rev. Earth Planet. Sci.*, *14*, 493–571, 1986.

J. Ita, Department of Geology and Geophysics, University of California, Berkeley, CA 94720.

L. Strixrude, Center for High Pressure Research, Geophysical Laboratory, Carnegie Institution of Washington, 5251 Broadbranch Road, N.W., Washington, DC 20015-1305.

(Received August 12, 1991;
revised December 23, 1991;
accepted December 27, 1991.)